

NAVAL POSTGRADUATE SCHOOL MONTEREY, CALIFORNIA



THESIS

EXPERIMENTAL PERFORMANCE STUDIES OF A PLATE HEAT EXCHANGER

by

Darren Plath

December, 1996

Thesis Advisor:

Ashok Gopinath

Approved for public release; distribution is unlimited.

DTIC QUALITY INSPECTED

19970623 064

REPORT DOCUMENTATION PAGE			Form Approved OMB No. 0704-0188	
Public reporting burden for this collection of information is estimated to average 1 hour per response, including the time for reviewing instruction, searching existing data sources, gathering and maintaining the data needed, and completing and reviewing the collection of information. Send comments regarding this burden estimate or any other aspect of this collection of information, including suggestions for reducing this burden, to Washington Headquarters Services, Directorate for Information Operations and Reports, 1215 Jefferson Davis Highway, Suite 1204, Arlington, VA 22202-4302, and to the Office of Management and Budget, Paperwork Reduction Project (0704-0188) Washington DC 20503.				
1. AGENCY USE ONLY (Leave blank)	2. REPORT DATE December 96	3. REPORT TYPE AND DATES COVERED Master's Thesis		
4. TITLE AND SUBTITLE EXPERIMENTAL PERFORMANCE STUDIES OF A PLATE HEAT EXCHANGER		5. FUNDING NUMBERS		
6. AUTHOR(S) Darren Plath				
7. PERFORMING ORGANIZATION NAME(S) AND ADDRESS(ES) Naval Postgraduate School Monterey CA 93943-5000		8. PERFORMING ORGANIZATION REPORT NUMBER		
9. SPONSORING/MONITORING AGENCY NAME(S) AND ADDRESS(ES)		10. SPONSORING/MONITORING AGENCY REPORT NUMBER		
11. SUPPLEMENTARY NOTES The views expressed in this thesis are those of the author and do not reflect the official policy or position of the Department of Defense or the U.S. Government.				
12a. DISTRIBUTION/AVAILABILITY STATEMENT Approved for public release; distribution is unlimited.			12b. DISTRIBUTION CODE	
13. ABSTRACT (maximum 200 words) A plate and frame heat exchanger experimental test stand was developed. Using this test stand a performance analysis was conducted. The analysis consisted of evaluating the performance of the heat exchanger at varying flow rates and inlet temperatures, to develop an effectiveness-NTU and Log Mean Temperature Difference relationships, under steady state operation. The measured heat rates were compared to the heat rates provided by the manufacturer and good/bad agreement was found. Standard operating procedures for the test stand were developed and implemented.				
14. SUBJECT TERMS Plate Heat Exchanger.			15. NUMBER OF PAGES * 76	
			16. PRICE CODE	
17. SECURITY CLASSIFICATION OF REPORT Unclassified	18. SECURITY CLASSIFICATION OF THIS PAGE Unclassified	19. SECURITY CLASSIFICATION OF ABSTRACT Unclassified	20. LIMITATION OF ABSTRACT UL	

Approved for public release; distribution is unlimited

**EXPERIMENTAL PERFORMANCE STUDIES OF A PLATE HEAT
EXCHANGER**

Darren R. Plath
Lieutenant, United States Navy
B.A., Macalester College, 1990

Submitted in partial fulfillment of the
requirements for the degree of

MASTER OF SCIENCE IN MECHANICAL ENGINEERING

from the

**NAVAL POSTGRADUATE SCHOOL
December, 1996**

Author: _____

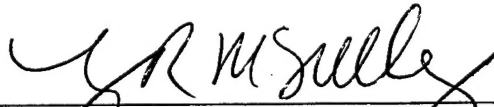


Darren R. Plath

Approved by: _____



Ashok Gopinath, Thesis Advisor



Terry R. McNelley, Chairman
Department of Mechanical Engineering

ABSTRACT

A plate and frame heat exchanger experimental test stand was developed. Using this test stand a performance analysis was conducted. The analysis consisted of evaluating the performance of the heat exchanger at varying flow rates and inlet temperatures, to develop an effectiveness-NTU relationship, under steady state operation. The measured heat rates were compared to the heat rates provided by the manufacturer and good/bad agreement was found. Standard operating procedures for the test stand were developed and implemented.

TABLE OF CONTENTS

I.	INTRODUCTION	1
II.	HEAT EXCHANGER DESCRIPTION	5
	A. GENERAL OVERVIEW	5
	B. PLATE DESCRIPTION	11
III.	EXPERIMENTAL APPARATUS	15
	A. PADDLEWHEEL FLOW SENSOR	15
	B. BAYONET-STYLE TANK HEATER	19
	C. SELF-PRIMING CENTRIFUGAL PUMP	20
	D. SYSTEM CONSTRUCTION	21
IV.	SYSTEM ALIGNMENT AND OPERATION	23
	A. INTRODUCTION	23
	B. SYSTEM ALIGNMENT	23
	C. OPERATING PROCEDURES	25
V.	DATA COLLECTION AND ANALYSIS	29
	A. APPROACH	29
	B. OVERALL HEAT TRANSFER COEFFICIENT	29
	C. THE EFFECTIVENESS-NTU METHOD	33
	D. LOG MEAN TEMPERATURE DIFFERENCE METHOD	35
VI.	DISCUSSION OF RESULTS	37
	A. INTRODUCTION	37
	B. OVERALL HEAT TRANSFER COEFFICIENT	37
	C. HEAT RATE	38
	D. HEAT EXCHANGER EFFECTIVENESS	39
VII.	CONCLUSIONS AND RECOMMENDATIONS	43
	APPENDIX A. STANDARD OPERATIONAL PROCEDURES FOR ALIGNMENT AND OPERATION OF THE SUPERCHANGER UX-056 PLATE AND FRAME HEAT EXCHANGERPLATE HEAT EXCHANGER .	45
	APPENDIX B. THERMOCOUPLE CALIBRATION	49
	APPENDIX C. UNCERTAINTY ANALYSIS	51
	APPENDIX D. EXPERIMENTAL DATA	55
	LIST OF REFERENCES	61
	INITIAL DISTRIBUTION LIST	63

LIST OF FIGURES

Figure 1. Superchanger Flow Diagram.....	6
Figure 2. Isometric Flow Diagram.....	7
Figure 3. Potential Leak Points.....	8
Figure 4. Plate Details.....	13
Figure 5. Cross Section of the FP-6000.....	16
Figure 6. FP-6000 Dimensions for Calculating "H" Dimension.....	17
Figure 7. Downstream Alignment using 10" Metal Rod.....	18
Figure 8. System Schematic Diagram.....	24
Figure 9. Plate Pack Thickness.....	26
Figure 10. NTU vs. Effectiveness.....	40
Figure 11. NTU vs. Effectiveness with error bars.....	41

LIST OF SYMBOLS

A_s	= Surface area [m ²]
c_p	= Constant pressure specific heat [J/Kg-K]
C	= Heat capacity rate
C_f	= Friction coefficient
C_r	= Heat capacity ratio
D_h	= Flow passage hydraulic diameter [m]
f	= Friction factor
k	= Thermal conductivity [W/m-K]
L	= Length in direction of flow [m]
\dot{m}	= Mass flow rate [Kg/s]
NTU	= Number of transfer units
Nu	= Nusselt number
Pr	= Prandtl number
\dot{Q}_{\max}	= Maximum possible heat transfer rate [W]
\dot{Q}	= Heat transfer rate [W]
Re	= Reynolds number
R_f	= Fouling factor
R_t	= Thermal resistance [K/W]
S	= Cross sectional area [m ²]
t	= Specified component thickness [m]
T_1	= Hot side inlet temperature [C]
T_2	= Hot side outlet temperature [C]
t_3	= Cold side inlet temperature [C]
t_4	= Cold side outlet temperature [C]
ΔT	= Change in temperature
U	= Overall heat transfer coefficient [W/m ² -K]
u	= Velocity [m/s]
α	= Convection heat transfer coefficient [W/m ² -K]
β	= Corrugation Angle
ϵ	= Effectiveness
μ	= Dynamic viscosity [N-s/m ²]
ν	= Kinematic viscosity [m ² /s]
ρ	= Density [Kg/m ³]

I. INTRODUCTION

The design of heat transfer equipment is and has been an interesting and important subject for some time. In the times of abundant and cheap energy, there was little incentive for industry to improve the performance of traditional heat exchangers. With ever increasing demands on a limited energy supply, the creation of more efficient and cost effective heat exchangers will play a more important role in society. Increased efficiency of heat transfer combined with cheaper manufacturing costs are two major factors in the design process of heat exchangers. A common design consists of a simple shell and tube configuration. These shell and tube heat exchangers are capable of handling a wide range of temperatures and pressures, while at the same time requiring a relatively large amount of space. An alternative design to the shell and tube heat exchanger that provides a large heat transfer area in a small volume is the flat plate and frame heat exchanger. As a general rule, the cost per unit surface area decreases with compactness. Flat plate and frame heat exchangers lend themselves to high effectiveness designs, thus promoting compactness. As a result, these heat exchangers are considered all around the world for many energy conservation and recovery applications.

Flat plate and frame heat exchangers are constructed of thin plates with relatively low thermal resistance. The plates are corrugated and packed close together forming small channels, thus taking advantage of the enhanced heat transfer associated with narrow passages. These heat exchangers can handle a wide range of fluids, from viscous to non-Newtonian. This ability to handle various fluids allows flat plate heat exchangers the potential for a wide variety of applications. These heat exchangers are used in the

automobile industry to control the temperature of paint and to cool automated welding machines. There are several other applications including the cooling of bleach solutions and boiler blow downs in the pulp and paper industry and process heating and cooling in the food industry. In beer breweries, plate and frame heat exchangers are used to cool the beer mixture before fermentation. Plate and frame heat exchangers are also used in chemical plants, power plants and on maritime shipping vessels.

The need for a heat exchanger that will resist corrosion and erosion by seawater is of prime concern for the Navy. Titanium plate heat exchangers have been found to be highly resistant to both conditions even at elevated velocities. In many cases the only required maintenance necessitated back flushing the units periodically. With the push to decrease manning on Naval vessels, any device that decreases maintenance is advantageous. As a result, numerous shell and tube electronic coolers have been replaced with Supercanger Navy standard heat exchangers throughout the fleet.

There are numerous advantages associated with flat plate heat exchangers. They are flexible, compact, have low fabrication costs, are easy to clean, afford increased protection against erosion and corrosion, provide temperature control with a small temperature difference required and have reduced fouling. The disadvantages are potential leakage through the gaskets, relatively high pressure drop through the heat exchanger and potentially high pumping costs. Another potential downfall of the flat plate heat exchanger is the limitation of temperature and pressure. If the temperature or pressure gets too high, there is a possibility of rupturing the gaskets resulting in leaks.

The purpose of this project was to produce a system design, component integration,

and to conduct a performance analysis of a Superchanger plate and frame heat exchanger. As part of the performance analysis, the overall heat transfer coefficient and the heat rate were derived both experimentally and theoretically and compared with each other. The heat transfer coefficient and other performance characteristics were then compared to the manufactures value.

The system consists of a Superchanger UX-056-UJ 23 plate and frame heat exchanger manufactured by Tranter inc., two 400 gallon water tanks, a bayonet-style tank heater from Cleveland Process Corporation, two Omega FP-6000 paddlewheel flow sensors, two single inlet centrifugal pumps powered by Baldor 2-Hp motors and various valves and piping. Inlet and outlet temperatures for both the hot and cold sides were measured with thermocouples. Numerous runs were conducted with various flow rates for both hot and cold sides to evaluate the heat exchanger performance.

II. HEAT EXCHANGER DESCRIPTION

A. GENERAL OVERVIEW

The plate and frame heat exchanger consists of a series of flow passages formed by corrugated heat transfer plates, a frame, nozzels, headers and tightening bolts. The corrugated plates are held in between the stationary and moveable frames and are compressed by the tightening bolts (Figure 2.1). The plates are equipped with elastomeric gaskets and have port holes pierced in the corners. When the unit is tightened, the gaskets seal the unit and, in conjunction with the nozzels and port holes, allows fluids to flow in alternate channels (A and B sides), thus putting the hot fluid and the cold fluid on opposite sides of the plate. [Ref. 1]. The dominating function of the headers is to uniformly distribute the fluids to the flow passages.

There are numerous advantages associated with plate heat exchangers. They are easy to assemble and disassemble, can be cleaned chemically and mechanically with minimal effort and the heat transfer area required can be changed simply with the addition or removal of plates. The plate exchanger can be used for multiple services at one time (Figure 2-2), floor space required is usually much less than that of a comparable shell and tube exchanger and very close temperature approaches can be obtained. In the case of a leak, since the unit is open and the gaskets vent to the atmosphere, the fluids will not mix and immediate detection is afforded. This can be seen in Figure 2-3. The figure shows three possible leak locations in which all the leaks are to the atmosphere. This is especially important when the mixing of the fluids could result in damage to machinery. Lube oil coolers are a prime

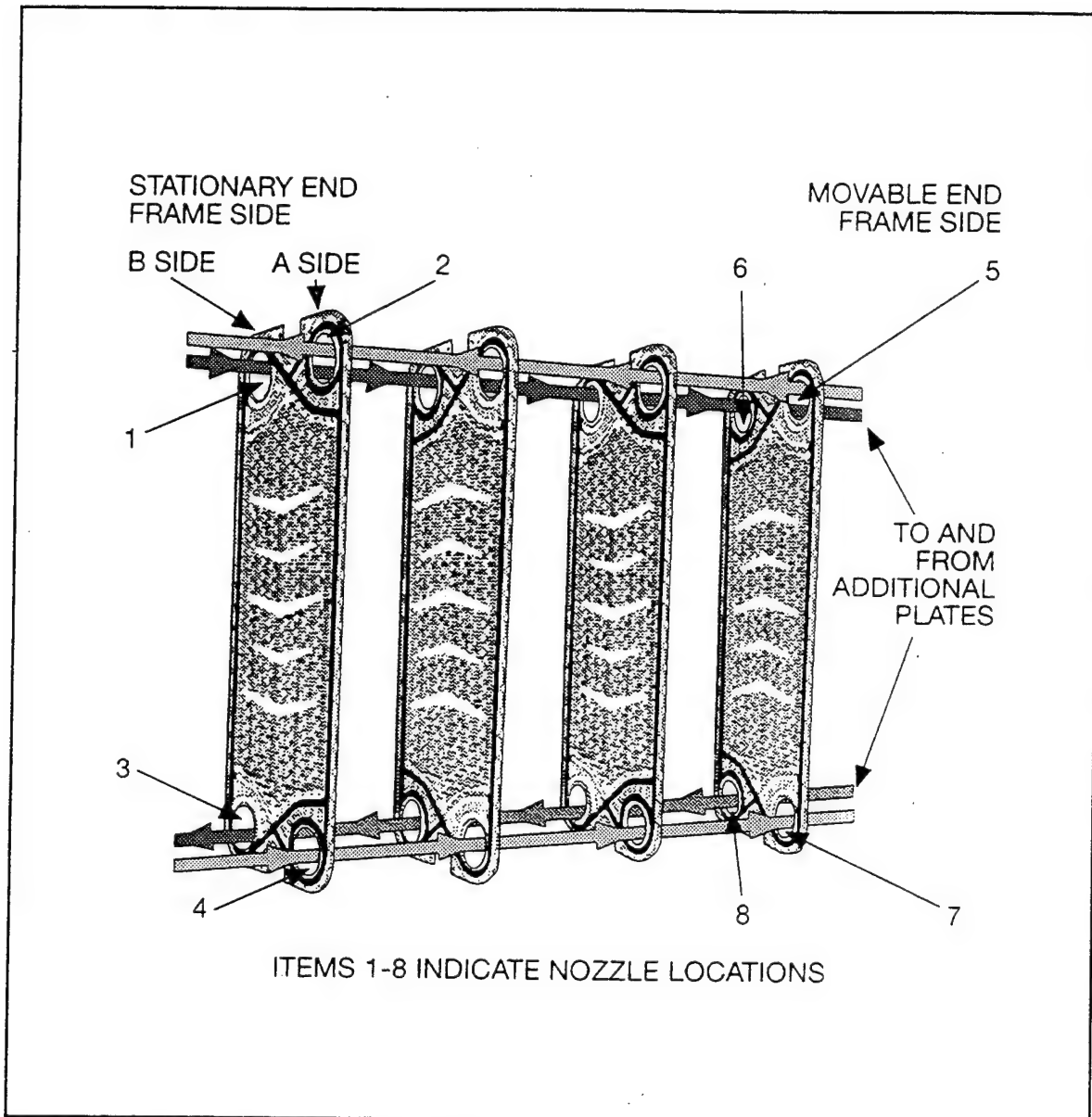


Figure 2.1 Supercharger Flow Diagram

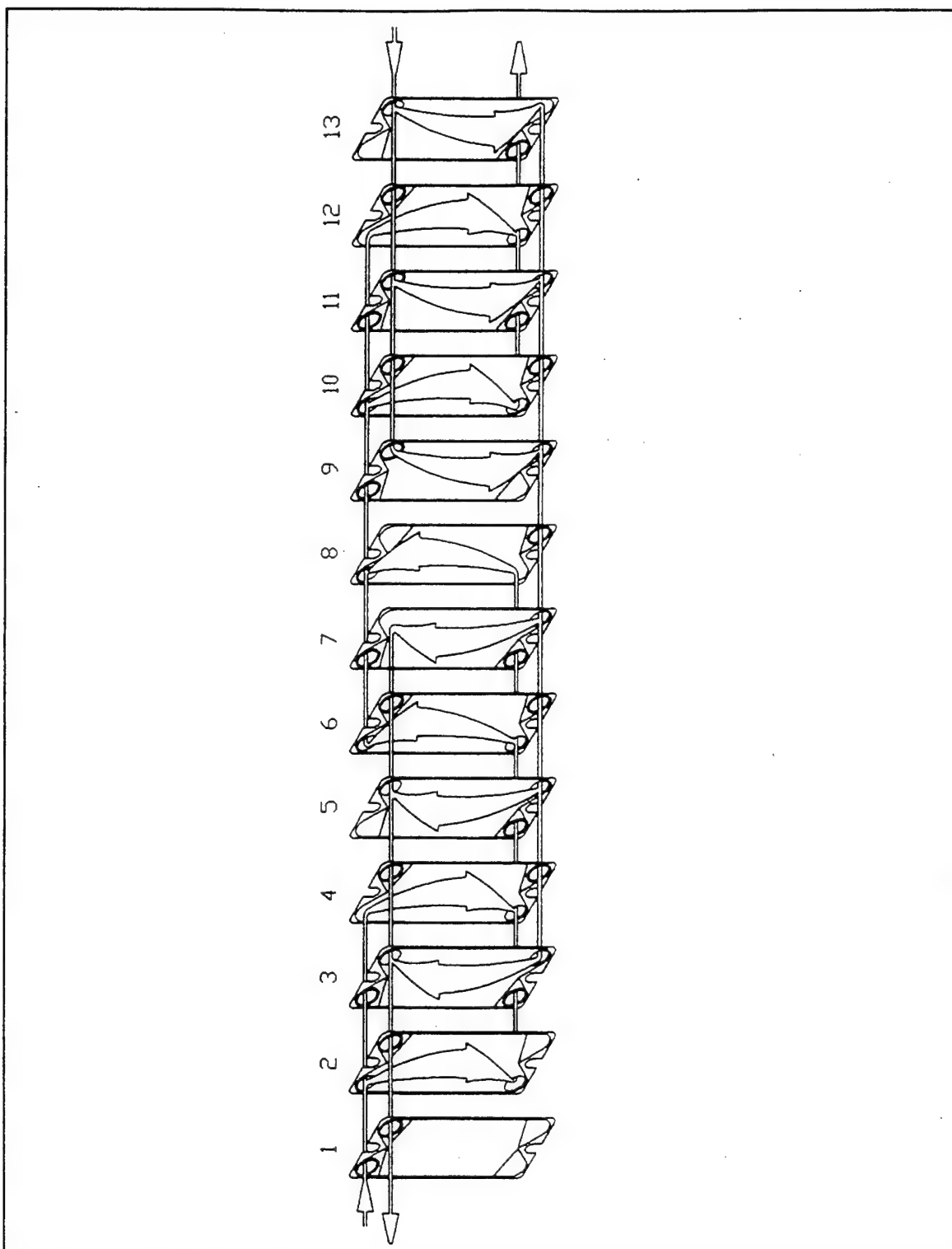


Figure 2.2 IsometricFlow Diagram

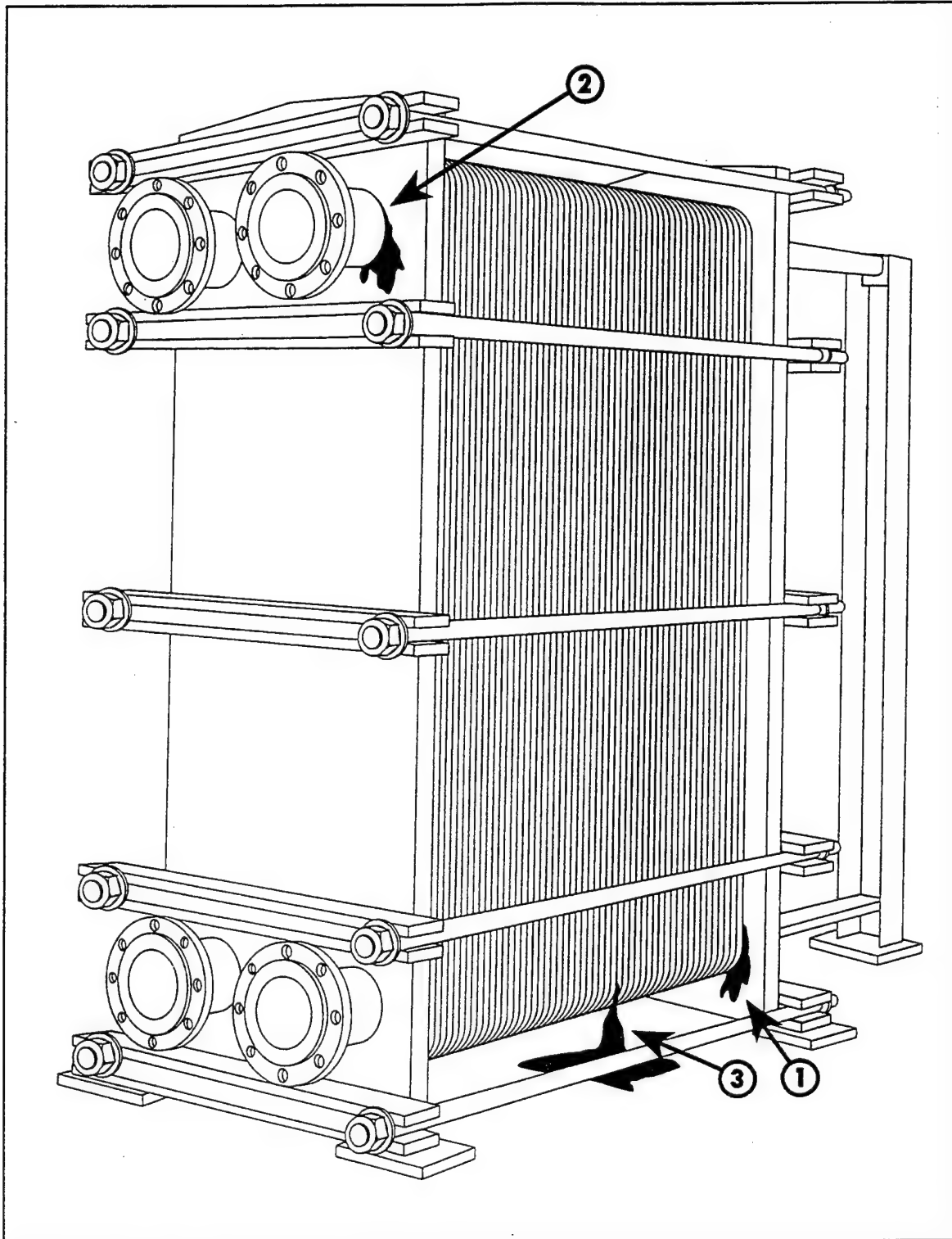


Figure 2.3 Potential Leak Points

example of this situation where the combining of oil and water is undesirable. Additional advantages are low hold up volume, stringent sanitary and hygienic conditions can be met, reduced fouling deposits even at low Reynolds numbers and when construction with other than carbon steel is required the plate exchanger can be more economical. Probably one of the most important advantages is the increased heat transfer coefficient that is obtained. This increased heat transfer coefficient leads to the requirement for less heat transfer area and in turn leads to more compact designs. [Ref. 2] Since the plates are very thin, the conduction resistance to heat transfer is minimal, thus providing an additional benefit.

In spite of all the advantages of the plate and frame heat exchanger there are also some disadvantages. The plate exchanger is limited by temperature and pressure. Temperatures must be maintained below 175 degrees celsius and pressures above 300 psi are unacceptable. These limitations are due to the gasket material seals, plate deformation and the frame. If the temperatures become too high, the gasket material and or the glue holding the gaskets could melt. This would lead to leakage in the heat exchanger. If the pressure was allowed to increase above the stated limits, the gaskets could be blown out of their retaining grooves and/or damage to the plates and frame could result.

Low flow rates, very viscous fluids, and fluids whose viscosity changes radically during passage through the unit should be avoided due to the possibility of maldistribution of the flow. Another disadvantage is the relatively high pressure drop that occurs in the exchanger. As a result, gas to gas service, air coolers and condensing duties can be limited as well. [Ref. 2]

As mentioned earlier, fouling is lower in plate heat exchangers. This is due to the

highly turbulent flows. This turbulence sustains small particles in suspension. The surface of each of the plates is very smooth, despite being corrugated which helps in reducing fouling deposits. There is low residence time for crystal formation and outstanding fluid dispersion with virtually no low velocity or dead zones. In addition the use of alloys that corrode at low rates can be utilized. This practically eliminates any corrosion products from fouling the heat exchanger. [Ref. 2]

The corrugations on the plates form narrow passages for the fluids to pass through, and the flow of the fluids is almost always countercurrent. The thin fluid interspace coupled with the corrugated plate design induces turbulence that produces extremely high heat transfer coefficients. [Ref. 1] The heat transfer coefficient, α , varies as a negative power of the flow passage size. A customary expression for the size of a non-circular flow passage is the *hydraulic diameter*, D_h , equaling four times the cross-sectional area divided by the wetted perimeter. Although a smaller hydraulic diameter increases friction, the benefits of compactness on the heat transfer coefficient generally outweigh the detrimental influence of small hydraulic diameter on friction. [Ref. 3]

In addition to the influence of small hydraulic diameter, increases in heat exchanger performance can be obtained by any modification of the surface geometry that results in a higher heat transfer coefficient at a given flow velocity. One widely accepted modification is the use of extended surfaces or fins, so that in addition to providing increased heat transfer surface area, the interrupted surface prevents the thickening of the fluid boundary layers. As the boundary layer develops, the heat transfer across the boundary layer decreases. Therefore, by reducing the boundary layers, the heat transfer is increased. Other methods of

obtaining increased performance by change of flow surface geometry include the use of curved, corrugated, or wavy passages, in which boundary layer separation and turbulence (promoters of heat transfer) are induced even at low Reynolds numbers. [Ref. 9] The method of corrugations is used in this plate and frame heat exchanger.

A common descriptor of compact heat exchangers is the *area density*, which is the ratio of heat transfer surface area to heat exchanger volume. A conventional cutoff for labeling a heat exchanger as compact is an area density value greater than 700 square meters per cubic meter (or 213 square feet per cubic feet). This is not a staunch rule however, as many heat exchangers have been grouped into the compact category with lesser area densities [Ref. 4]. It will be taken then that compact heat exchangers have a significantly increased area to volume ratio compared to that of an orthodox shell and tube unit. The compactness of these designs is derived through the need for an extended heat transfer area and in the use of plates instead of tubular heat transfer surfaces.

The corrugations also form contact points between adjacent plates. These contact points lend rigidity to the plates, helping them to withstand higher pressures and minimizing plate deflections.

B. PLATE DESCRIPTION

The plates are manufactured in standard sizes from die-formed sheet metal in virtually any material that can be cold worked. Since no welding is used, the weldability of the metal is not a concern. They are pressed out of a thin flat sheet of metal. The size,

number and arrangement of the plates is contingent upon the duty to be performed. This unit has plates with an area of 0.635 square feet per plate. The heat exchanger has 23 plates. Two of these plates are in a buffer zone, leaving 21 useable plates. The total heat transfer area of the heat exchanger is 13.3 square feet.

The fluids enter the heat exchanger through inlet nozzles and travel through the port holes in the plates. These port holes comprise the header. The individual fluids pass through alternating plates in opposite directions. [Ref. 1] Typical plate thicknesses range from .5 to 1mm. The material used for the plates is chosen on the basis of pressure and corrosion conditions. For this plate and frame heat exchanger the plates are made of 316 stainless steel and are 0.023622 inches (0.6 mm) thick.

The corrugations are in a herringbone or chevron pattern (Figure 2-4) and are inclined at an angle β to the direction of flow. The angle β of the unit tested is 60 degrees. Also shown in the figure is an alternate washboard plate design. As the angle of inclination changes, so does the resulting heat transfer coefficient and the friction factor. The heat transfer coefficient increases with β up to an angle of approximately 75 degrees from vertical. The friction factor increases by about ten times with an angle change from 30 to 75 degrees. [Ref. 5] These corrugations are designed to increase the Nusselt number thus providing enhanced fluid heat transfer. The heat transfer enhancement of the corrugations is due to induced turbulence in the flow. The turbulence eliminates stagnant areas in the liquid flow. Since there are no places for the fluids to collect, all of the plate is used, thus increasing the effective heat transfer area of the heat exchanger. An additional benefit of the corrugations is the added mechanical support to the plate. When an adjacent plate with its chevron pattern

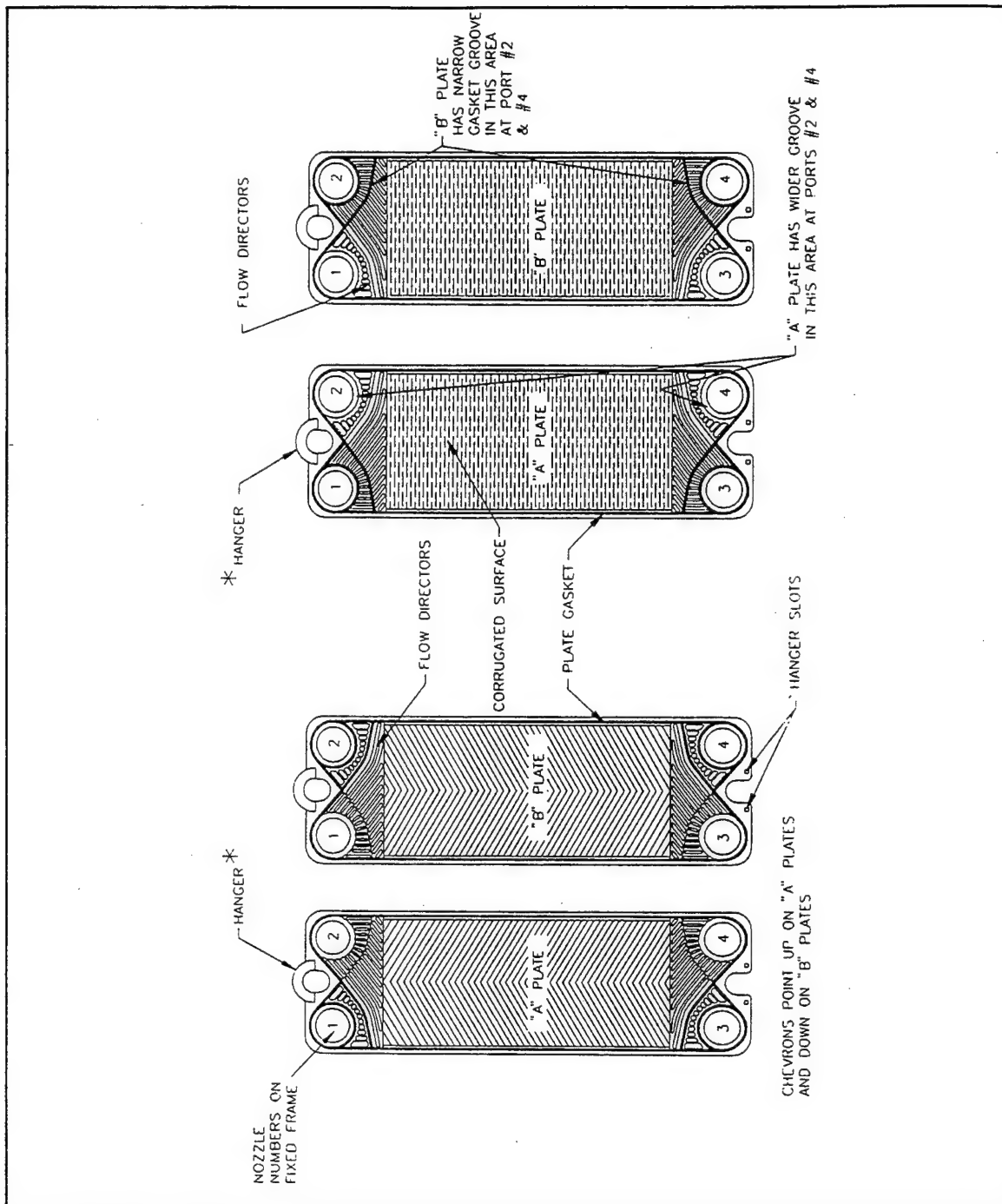


Figure 2.4 Plate Details

reversed is stacked together, multiple contact points are created. These multiple contact points provide support for the thin plates and increase the heat transfer between the hot and cold sides of the heat exchanger. [Ref. 1]

There is a groove around the circumference of the plate which accepts the sealing gasket. Due to the ribbed nature of the groove, additional reinforcement is added to the plate. The gaskets are a single piece of material, has a molded construction, and is generally bonded to the plates with Pliobond 30 adhesive. The gasket material is NBR and is selected based on the compatibility with operating temperatures and the fluids being processed.

Fluid passage holes are pierced at the corners of each plate. The number and location of holes is dependent on the location of the plate in the heat exchanger. Flow directors are located at the top and bottom of the heat transfer surface in the port hole areas which evenly distribute the fluids. When the heat exchanger is put together, the combination of fluid passage holes on the plates comprise a flow path for the fluids. The plates can be arranged in a variety of ways depending on the number of passes required.

III. EXPERIMENTAL APPARATUS

A. PADDLEWHEEL FLOW SENSOR

The flow sensor chosen for this experimental analysis was the Omega FP-6000 (Figure 3-1). The fluid flowing by the sensor rotates the paddlewheel. As each blade of the paddlewheel passes the magnet in the transducer, it causes a change in the magnetic flux field running through the coil and core. When this flux field changes, an alternating current (AC) voltage, approximating a sine wave, is induced. The frequency of the output voltage of the coil is directly proportional to the linear velocity of the fluid in the pipe; therefore, it represents the amount of fluid passing the flow sensor in a particular increment of time. A complete cycle occurs each time one of the paddlewheel blades passes the coil; therefore, four complete cycles are generated for each paddlewheel rotation. The FP-6000 senses local velocity at an insertion depth of 10% of inside diameter, therefore, the velocity that it detects is approximately 95% of the mean velocity in the pipe. The flow sensor is constructed of brass and is completely self contained with out any user serviceable parts. [Ref. 6]

Installation of the flow sensor started with the calculation of the "H" dimension (Figure 3-2). The following equation was used:

$$H = 5.95 - \text{wall thickness} - 10\% \text{ of inner diameter} \quad (3.1)$$

The "H" dimension was found to be 5.55 inches. Next the sensor was located in an undisturbed section of pipe at the twelve o'clock position just prior to the entrance to the plate heat exchanger. The lower hex nuts were adjusted to allow the moving of the flow sensor to the calculated "H" dimension. The jam nuts were tightened securing the sensor.

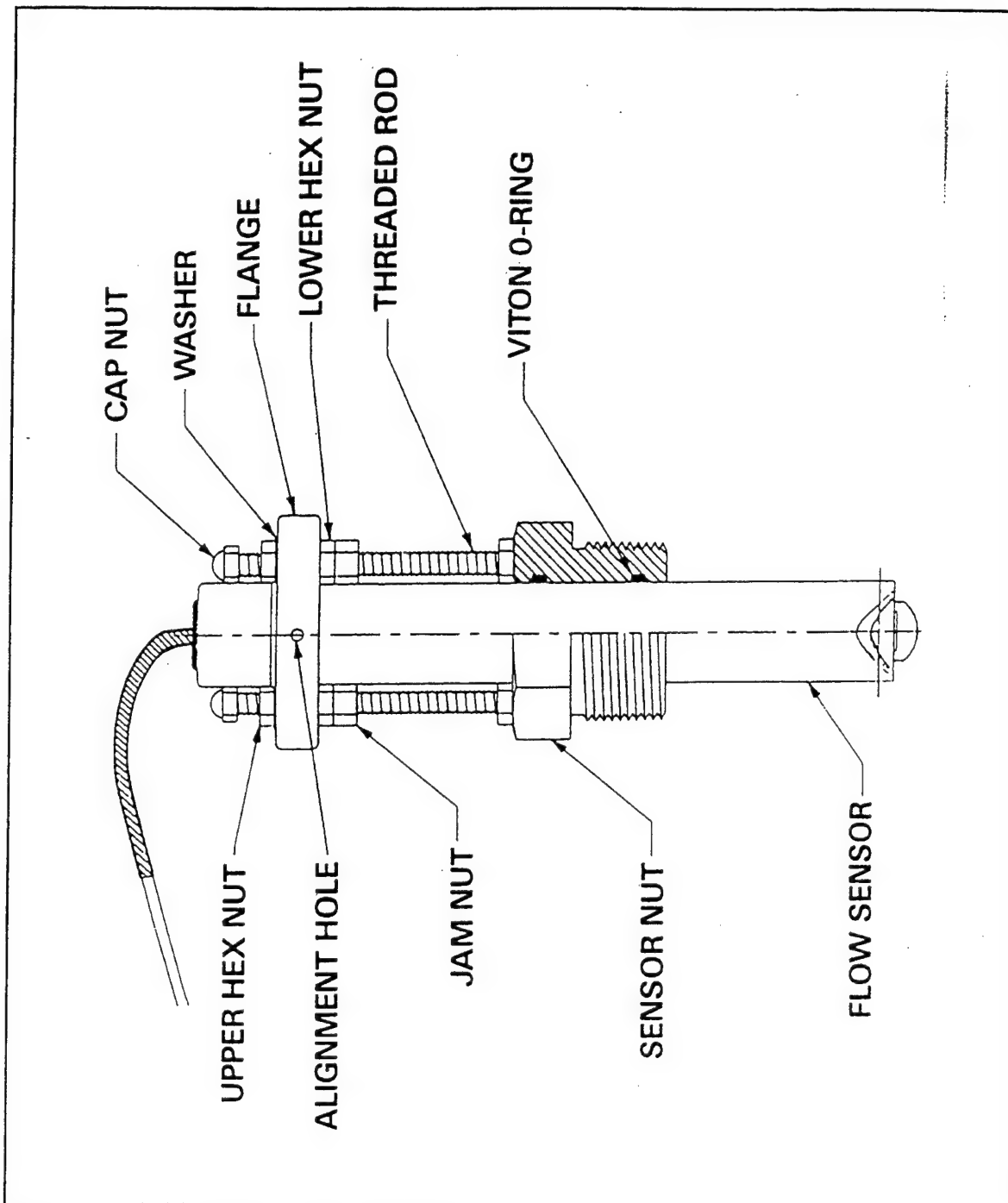


Figure 3.1 Cross Section of the FP-6000

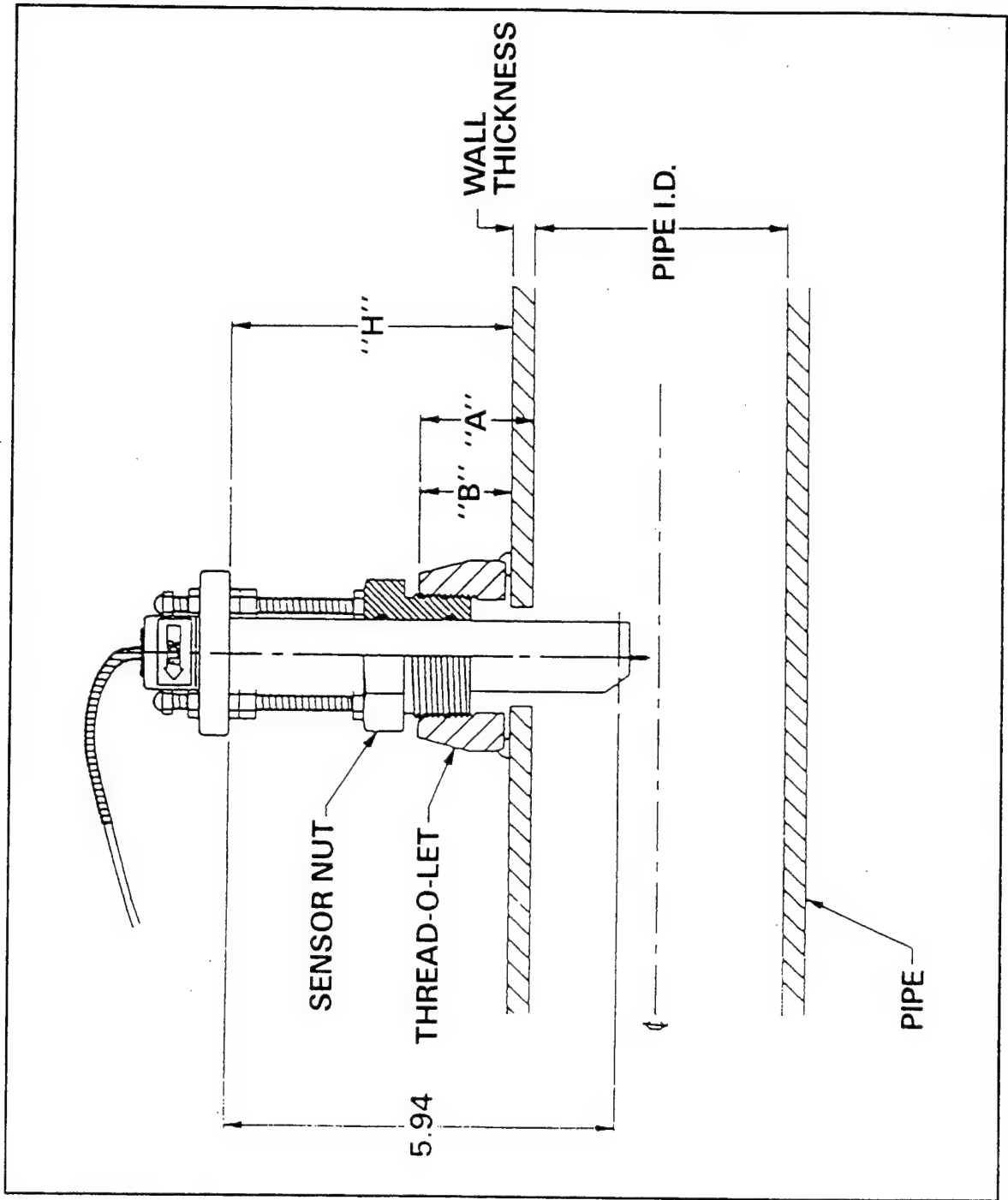


Figure 3.2 FP-6000 Dimensions for Calculating "H" Dimension

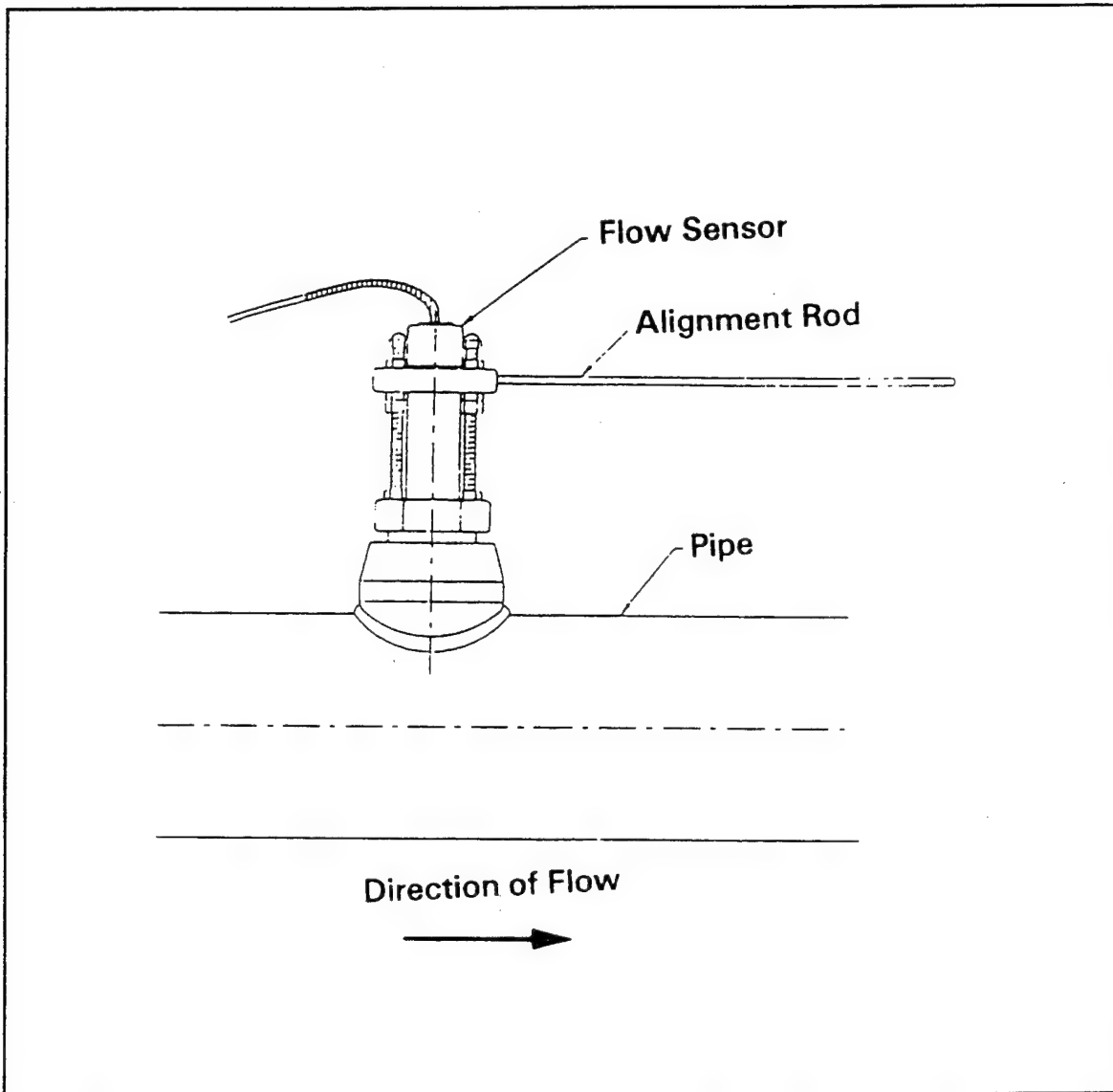


Figure 3.3 Downstream Alignment using 10" Metal Rod

The sensor was then inserted in the saddle fitting with the alignment hole on the flange pointing in the down stream direction of the flow. A ten inch rod was provided with the flow sensor to make minor adjustments to the alignment of the sensor (Figure 3-3). The wire leads from the flow sensors were fitted with BNC plugs. A digital frequency reader was used to measure the flow rates.

B. BAYONET-STYLE TANK HEATER

In order to achieve a sufficient temperature difference, an immersion style tank heater was used. A Cleveland Process Corporation Bayonet-style immersion tank heater was selected. The heater is constructed of 304 stainless steel, has three elements, is three phase 480 volts, and 27,000 watts. The heater has an auto shut off device incase a low water situation arises. A bracket was manufactured to hang the tank heater in the middle of the tank. The bayonet-style tank heater is 51 inches in length. The hot zone extends 42 inches from the bottom.

The required heat rate of the heater was determined using the following equation:

$$\dot{Q} = m C_p \Delta T \quad (3.2)$$

The mass of the water was calculated by multiplying the volume of the tank with the density of water at room temperature. Room temperature was taken to be 22 degrees Celsius. The temperature difference used in the previous equation is, the difference in temperature between the water leaving the tank and that of the water returning to the tank. A maximum

temperature difference of 10 to 15 degrees is expected. With ΔT set at the upper limit of 15 degrees, the resulting heat rate Q , is 113.452 MJ. While this requirement is larger than the heater selected, it is assumed that over a relatively short duration, the temperature will remain fairly constant in the tank. Since the tank is rather large and the heater is located between the returning water and the out going water, this assumption should be valid. It is noted that the majority of runs will be conducted with the delta T being less than 15 degrees. In addition, as the flow rate increases, the time duration of constant temperature will decrease.

C. SELF-PRIMING CENTRIFUGAL PUMP

Two single inlet centrifugal pumps powered by Baldor 2-Hp motors were chosen for this experimental performance analysis. The pumps are self priming and are designed for continuous transfer pumping of liquid from tanks or sumps. Each pump has twelve feet of suction lift. The motor operates at 3450 RPM, 115 volts and 60 Hz.

A preliminary system headloss calculation was conducted using the Darcy-Wiesbach equation:

$$H_f = f \frac{L}{D} \frac{u^2}{2g} \quad (3.3)$$

Minor losses were also accounted for. K values for 90 degree elbows were taken to be 1.4, for valves k equaled 0.26. [Ref. 7] The pressure drop through the heat exchanger used was 6 psi (from manufacturer). Measurements of pipe lengths and number of elbows and valves

were taken from the preliminary system diagram. The piping used was schedule 40 PVC. The pipe is considered smooth and a friction factor of 0.015 was used. The head loss calculated was 32.64 ft of water.

In planning the performance analysis, it was decided that a wide range of flow rates would be desirable. Cross referencing several vendor catalogs provided us with several options to choose from. The pump chosen, is capable of providing 115 gpm at 35 ft of head. This is more than sufficient for this experimental performance analysis.

D. SYSTEM CONSTRUCTION

The experimental apparatus started with a preliminary piping diagram. From this diagram measurements were taken to calculate the length of pipe and the number of valves required. Piping, valves and assorted other items were then purchased. The two water tanks were cleaned and positioned in the laboratory. Once all items were received construction began.

The first step involved drilling holes in the floor to secure one of the pumps in place. The inlet piping was then connected. Each threaded connection was wrapped with teflon tape, to protect against the possibility of leaks. Non-threaded connections were sanded, primed and then glued together. The next step was to hook up the discharge of the pump to the inlet of the heat exchanger. The paddlewheel flow sensor and thermocouple bead were inserted in this section. A recirculation line was also installed. Next a line was connected from the discharge of the heat exchanger to the tank. This completed one side of the heat exchanger setup. The other side was identical. The paddlewheel flow sensors were then

positioned according to the operating instructions. Before the thermal couple beads were inserted to the system, they were calibrated. The thermocouple calibration is discussed in Appendix B.

IV. SYSTEM ALIGNMENT AND OPERATION

A. INTRODUCTION

The objective of this chapter is to discuss the basic philosophy and decision making process used in developing the Standard Operational Procedures for the plate and frame heat exchanger system. The primary goal in the development of the standard operational procedures was to produce a detailed step by step procedure which can be followed by an operator with a general knowledge of the overall system. The major criteria are both safety of the operator and to prevent damage to equipment. Two procedures have been developed to help accomplish the above goals. They are listed below:

- * Heat Exchanger System Recirculation Procedure (HESRP)

- * Heat Exchanger System Operational Procedure (HESOP)

The above written procedures are contained in Appendix A.

B. SYSTEM ALIGNMENT

As mentioned earlier the experimental apparatus consists of two water tanks, two centrifugal pumps, two paddlewheel flow sensors and a plate and frame heat exchanger. A schematic diagram of the system is shown in figure 4-1. The hot and cold sides of the system are exactly the same with the exception of valve numbering. HW and CW will be used to denote the hot and cold side valves respectively. For this reason, only one side will be discussed.

The flow path of the water will be described starting at the water tank. Water flows

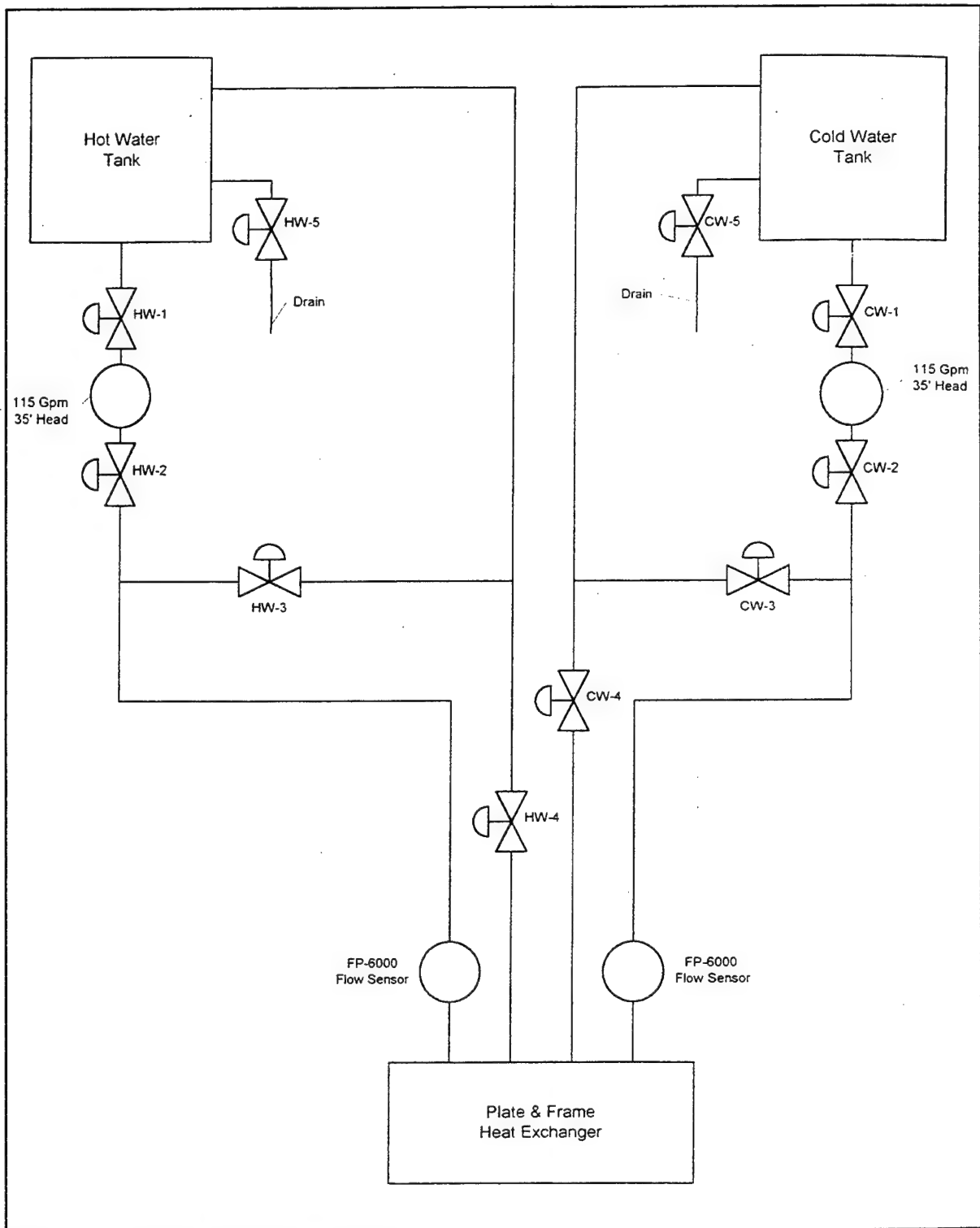


Figure 4.1 System Schematic Diagram

through the pump suction valve HW-1 into the centrifugal pump. From the pump it flows through the discharge valve HW-2. After this valve the line branches in two. One branch is a recirculating line back to the tank. This recirculation line will allow for increased mixing of the fluid in the tank prior to each test run. This mixing will help allow the assumption of a constant temperature throughout the tank to be valid. The other line continues toward the heat exchanger. The water passes through the paddlewheel flow sensor and into the heat exchanger unit. After traversing the heat exchanger the fluid passes through valve HW-4 and then back to the tank. Valves HW-4 and CW-4 will serve as throttle valves, permitting the capability to increase or decrease the flow rates as necessary. Temperature measurements are taken prior to entering and upon exiting of the heat exchanger as well as in both tanks.

C. OPERATING PROCEDURES

The procedure starts with a safety space walk through, system verification and system alignment. During the visual inspection of the heat exchanger lab space, emphasis is placed on removing water and any debris from the area, as well as, checking for leaks and damaged equipment. After completion of the safety walk through the operator commences with placing the system in recirculation mode. The operation of the system is quite simple, however the correct valves must be open for the water to flow through the heat exchanger. Damage to the heat exchanger could result from improper operation.

The first step is to turn on the heater. The water must be heated to the desired starting temperature. Before allowing any fluid to flow the operator must ensure the plate pack

length is correct. The maximum length is 2.9 inches and the minimum length is 2.7 inches.

Figure 4-2 shows the plate pack thickness as the dimension "A". Once the water has reached

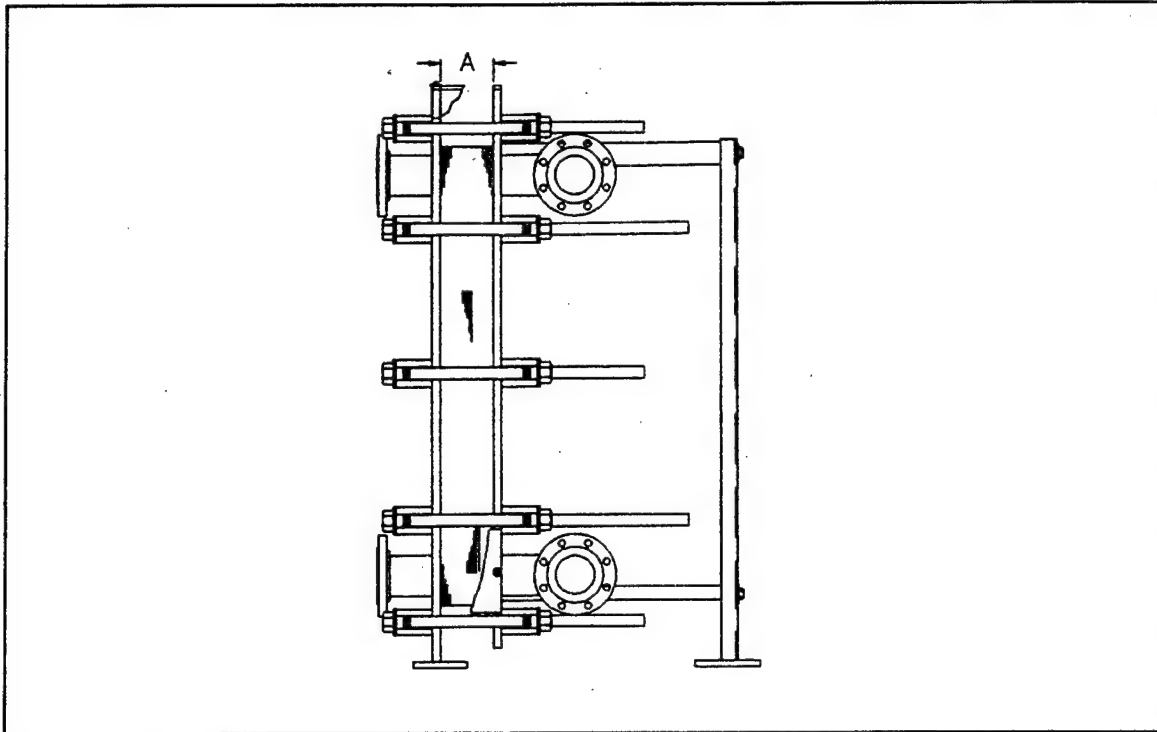


Figure 4.2 Plate pack thickness

the required temperature, the pumps can be aligned for operation. The operator will first place the system into a recirculation mode in accordance with procedure (HESP) in Appendix A. The following paragraph gives a brief explanation of this procedure.

Ensure that both HW-1 and CW-1 are open. Second, close valves HW-2 and CW-2 and open valves HW-3 and CW-3. Next check to see that valves HW-4 and CW-4 are closed. As a reminder both drain valves HW-5 and CW-5 are to remain closed at all times during the experimental analysis. The next step is to start both pumps. Once both pumps have been started, slowly open the discharge valves HW-2 and CW-2. This will allow the fluid to flow through out the sytem in a recirculating mode.

When ready to proceed with the experimental analysis, the operator will place the system in operation in accordance with procedure (HESOP) Appendix A. Slowly open valves HW-4 and CW-4. Open the cold side first. This will ensure that cooling water is flowing through the heat exchanger prior to the hot fluid. For this experimental analysis, the cold fluid is room temperature water. Since the heat exchanger will be at room temperature this procedure will reduce the possibility of any thermal shock or over heating of the heat exchanger. Now that the system is in operation, use valves HW-4 and CW-4 to adjust the flow rate through the heat exchanger.

It is important to monitor the system for any possible leaks that may occur. In the case of a leak, the operator needs to identify which side of the system it has occurred on. If a leak occurs, slowly shut both pump discharge valves HW-2 and CW-2, then stop the pumps. Ensure corrective measures have been completed before operating the system again.

V. DATA COLLECTION AND ANALYSIS

A. APPROACH

In conducting the performance analysis of the plate and frame heat exchanger, the Effectiveness - NTU and Log Mean Temperature difference methods were utilized. The major requirement for these methods is the determination of a heat exchanger overall heat transfer coefficient. This includes the computing of other parameters such as the hot and cold side convection coefficients, wall conduction resistance, and fouling resistance. The overall heat transfer coefficient was found both from theoretical and experimental data. Since low fouling factors are an inherent advantage of plate and frame heat exchangers, the calculation of a fouling resistance will be neglected, however the negative impact of fouling will be discussed.

B. OVERALL HEAT TRANSFER COEFFICIENT

1. Newton's Law of Cooling

The total thermal resistance to heat transfer between two fluids separated by a heat exchanger structure is termed the *overall heat transfer coefficient*, U . The determination of U is essential to any heat exchanger analysis. In an expression analogous to Newton's Law of Cooling, the heat transfer between two fluids separated by one or more thermal resistances, R_p , is:

$$\dot{Q} = \frac{\Delta T}{\sum R_t} = UA_s \Delta T \quad (5.1)$$

The result apparent from the above expression, that $1/\sum R_f = UA_s$, is applicable to clean, unfinned surfaces only, but can be used as the basis for determining a heat exchanger's overall heat transfer coefficient with additional factors considered such as the effects of wall conduction and the presence of fouling on both hot and cold water sides. As mentioned earlier, the effects of fouling will be neglected in the calculations. [Ref. 8]

2. Convection Coefficients

The water side *convection coefficients*, α_h and α_c , are computed in the following manner as recommended in Hewitt's Process Heat Transfer. [Ref. 5]

(1) Mass Flow Rate. The mass flow rate per passage is found from the following equation:

$$\dot{m} = \frac{2\dot{M}}{N + 1} \quad (5.2)$$

where, \dot{M} is the total mass flow rate of the system.

(2) Cross Sectional Area. The cross sectional area of each passage is given by:

$$S = bW \quad (5.3)$$

where b is the gap between plates and W is the width of the plate.

(3) Water Velocity. The water velocity across the plate is given by:

$$u = \frac{\dot{m}}{\rho S} \quad (5.4)$$

(4) Reynolds Number. The *Reynolds number*, Re , can be computed using the following relation:

$$Re = \frac{uD_h \rho}{\mu} \quad (5.5)$$

(5) Nusselt Number. The approximation for the *Nusselt Number*, Nu , in the turbulent region is

$$Nu = 0.4 (Pr)^{0.4} (Re)^{0.64} \quad (5.6)$$

(6) Convection Coefficient. The convection coefficient can now be found using the following relation:

$$\alpha = \frac{kNu}{D_h} \quad (5.7)$$

where k , is the thermal conductivity of the fluid.

(7) Sequence of Computations. Computations of the convection coefficients for each side of the system's heat exchanger were completed, and are shown as part of Appendix D.

3. Fouling Resistance

During normal heat exchanger operation, surfaces are often subject to fouling by fluid impurities, rust or scale formation, and other reactions between the fluid and the wall

material. Depositions such as these can greatly increase the resistance to heat transfer between the fluids. This effect can be treated by introducing an additional thermal resistance, termed the *fouling factor*, R_f , the value of which depends on the operating temperature, fluid velocity, and length of service of the heat exchanger. The heat exchanger used is brand new and the amount of fouling expected is extremely small. Since the values for the fouling factor are very small compared to the convection coefficients and the thermal resistance of the plates, they can be neglected.

4. Plate Conduction

Derivations of the *plate conduction resistance*, R_{wall} by Incropera and DeWitt [Ref.7] produce the following expression for heat exchanger plates (modeled as plane wall):

$$R_{wall} = \frac{t}{k} \quad (5.8)$$

where t is the plate thickness and k is the thermal conductivity of the plate.

5. Summation of Elements

The summation of thermal resistances including effects of hot and cold side convection, and plate conduction yields the following:

$$\frac{1}{U} = \frac{1}{\alpha_h} + R_{wall} + \frac{1}{\alpha_c} \quad (5.9)$$

The area is not included in equation 5.9 since the area is the same for both sides of the plate.

C. THE EFFECTIVENESS - NTU METHOD

1. Applicability

The *Effectiveness - NTU* method utilizes the overall heat transfer coefficient to determine heat exchanger heat transfer performance characteristics. In the Effectiveness - NTU approach, with knowledge of the heat exchanger type, size, and fluid flow rate, the NTU, *maximum heat transfer rate*, \dot{Q}_{\max} , and *effectiveness*, ϵ , the actual heat transfer rate can be determined.

2. Maximum Possible Heat Transfer Rate

The maximum possible heat transfer rate for a given heat exchanger is achieved when, by definition, the entering cold fluid temperature reaches the maximum possible temperature difference, i.e., that of the entering hot fluid temperature. Using capital T for the hot stream and little t for the cold stream, then T1 and T2 correspond to the entrance and exit temperatures of the hot stream respectively. Alternately, t3 and t4 correspond to the entrance and exit temperatures of the cold stream respectively. Thus the entering cold fluid would rise in temperature by the quantity $(t_4 - t_3)$. The heat transfer rate can be found using the following relationship:

$$\dot{Q} = \dot{m}c_p(t_4 - t_3) \quad (5.10)$$

where the term $\dot{m}c_p$ is defined as the *heat capacity rate*, C , and will be based on the mass flow rate, \dot{m} , and specific heat, c_p , of the fluid. The *maximum heat transfer rate*, \dot{Q}_{\max} ,

is then:

$$\dot{Q}_{\max} = C_{\min}(T_1 - t_3) \quad (5.11)$$

where C_{\min} is equal to either C_{hot} or C_{cold} , whichever is smaller. [Ref. 8]

3. Effectiveness

The *effectiveness*, ϵ , is defined as the ratio of the actual heat transfer rate for a heat exchanger to the maximum possible heat transfer rate.

$$\epsilon = \frac{\dot{Q}}{\dot{Q}_{\max}} \quad (5.12)$$

The effectiveness, which is dimensionless, must be in the range $0 \leq \epsilon \leq 1$. [Ref. 5]

It is useful because, if ϵ , T_1 , and t_3 are known, the actual heat transfer rate may be

determined from the expression:

$$\dot{Q} = \epsilon \dot{Q}_{\max} = \epsilon C_{\min}(T_1 - t_3) \quad (5.13)$$

4. Number of Transfer Units

The *number of transfer units*, NTU , as explained by Incropera and Dewitt [Ref. 8], is a dimensionless parameter that is widely used for heat exchanger analysis and is defined as:[Ref.5]

$$NTU = \frac{UA_s}{C_{\min}} \quad (5.14)$$

5. Effectiveness - NTU Relations

The Effectiveness - NTU relationship for the type of heat exchanger being analyzed, i.e. a single pass counter flow plate heat exchanger with both fluids unmixed is:

$$\epsilon = \frac{\exp [(1 - C_r) NTU_{\min}] - 1}{\exp [(1 - C_r) NTU_{\min}] - C_r} \quad (5.15)$$

where:

$$C_r = \frac{C_{\min}}{C_{\max}} \quad (5.16)$$

D. THE LOG MEAN TEMPERATURE DIFFERENCE METHOD

The log mean temperature difference method makes use of parameters such as the inlet and outlet temperatures and the mass flow rate of the fluids. With inlet and outlet temperatures and mass flow rates known, the heat rate can be obtained by applying overall energy balances to the hot and cold fluids. If \dot{Q} is the total rate of heat transfer between the hot and cold fluids and there is negligible heat transfer between the exchanger and its surroundings, as well as negligible potential and kinetic energy changes, application of an energy balance gives:

$$\dot{Q} = \dot{m}_h C_{p_h} (T_{h,i} - T_{h,o}) \quad (5.17a)$$

and

$$\dot{Q} = \dot{m}_c C_{p_c} (T_{c,i} - T_{c,o}) \quad (5.17b)$$

where the temperatures appearing in the expressions refer to mean fluid temperatures at the

designated locations. [Ref. 8]

Another way of looking at the relationship between the total heat transfer rate \dot{Q} and the temperature difference, ΔT , is:

$$\dot{Q} = UAF\Delta T_{lm} \quad (5.18)$$

where ΔT_{lm} is an appropriate mean temperature difference and F is a correction factor to account for the non-counter flow configuration. The correction factor, F , is a function of the ratio of mass flow rates, temperature differences and heat exchanger configuration. The value for F was taken to be 0.96 for this particular heat exchanger. [Ref. 5] For plate heat exchangers with countercurrent flow and both fluids unmixed, the form of ΔT_{lm} is as follows:

$$\Delta T_{lm} = \frac{(T_{h,i} - T_{c,o}) - (T_{h,o} - T_{c,i})}{\ln \frac{T_{h,i} - T_{c,o}}{T_{h,o} - T_{c,i}}} \quad (5.19)$$

From equation 5.18 the overall heat transfer coefficient can be found using equations 5.17 and 5.19.

VI. DISCUSSION OF RESULTS

A. INTRODUCTION

From the data collected three important heat exchanger parameters were calculated and compared in this experimental study. They are the overall heat transfer coefficient, heat exchanger effectiveness and the heat rate. All values were first calculated from correlations recommended by Hewitt in Process Heat Transfer [Ref. 5] and then from the measured experimental data. A detailed discussion of these parameters follows.

B. OVERALL HEAT TRANSFER COEFFICIENT

With knowledge of the mass flow rate and the inlet temperatures of the hot and cold fluids, the Reynolds number, Nusselt number and finally the convection coefficient for both the hot and cold sides of the heat exchanger were calculated from available correlations. The convection coefficients along with the plate conduction comprise the overall heat transfer coefficient. This gives us the expected value of the overall heat transfer coefficient.

The overall heat transfer coefficient was also found by experimentation using the log mean temperature difference method. Using the simple energy balance of equations 5.17a and 5.17b the heat rate for the hot and cold sides were computed. With the known inlet and outlet temperatures along with the heat rate obtained, equation 5.18 can be used to obtain UA . The value of F was given earlier to be 0.96. The log mean temperature difference was computed using equation 5.19.

The experimental values for the overall heat transfer coefficient were approximately 15 -20% lower than the expected values. This can be attributed to using an a correlation for

the Nusselt equation based on a standard plate exchanger and from the extraction of the experimental heat transfer coefficient from the energy balance. The Nusselt correlation could produce a slightly higher value while the energy balance yields a lower value. The energy balance will be discussed in the heat rate section.

All calculations were performed in a spreadsheet and are included as Appendix D.

C. HEAT RATE

The heat rate was calculated in two different ways. The first utilized the Log Mean Temperature Difference method, and the second finds the heat rate using the simple energy balance. Using the value of the overall heat transfer coefficient calculated earlier, and equation 5.18, with the area provided by the manufacture and the correction factor discussed earlier, the expected value of the heat transfer rate can be obtained.

The second method used to acquire the heat rate was the energy balance equations of 5.17a and 5.17b. In principle, the heat transfer from one fluid must equal the heat transfer to the other fluid. The heat rates for the cold and hot fluids were compared and found to be well within the estimated uncertainty limits. The uncertainty ranged from a low of 4.62% to a high of 28.38%. The high value of uncertainty is attributed to cases of large disparity between the flow rates of the hot and cold fluid streams. For the most part the values were within 10% of each other.

The experimental heat rate values were less than the expected estimates. A small portion of the difference can be accounted for by the assumption that all the heat is transferred between the fluids. This assumption is not entirely true since some heat is lost through the heat exchanger to the surroundings. A standard fin analysis was conducted on

the heat exchanger and it was discovered that the losses were on the order of 100 watts. A second assumption used was that the fluids are evenly distributed between the channels. It was also assumed that the heat exchanger was in steady state operation.

D. HEAT EXCHANGER EFFECTIVENESS

As seen in figure 6-1, the effectiveness-NTU relationship in equation 5.15 is used to produce the solid and dotted line curves for increasing C_r with the lower bound having a C_r value of .999 and the upper bound value of 0. The experimental data fits within these bounds very nicely. The dots correspond to values of C_r between 0.97 and 0.99 while the triangles correspond to various C_r values ranging from 0.17 to 0.80. It can be seen from figure 6-1 that the theoretical values obtained from the effectiveness NTU relation correlate well to the experimental data. Figure 6.2 shows the same Effectiveness-NTU plot with the experimental uncertainty superimposed as error bars. The larger uncertainties are due to large disparities in the flow rates.

NTU vs. Effectiveness

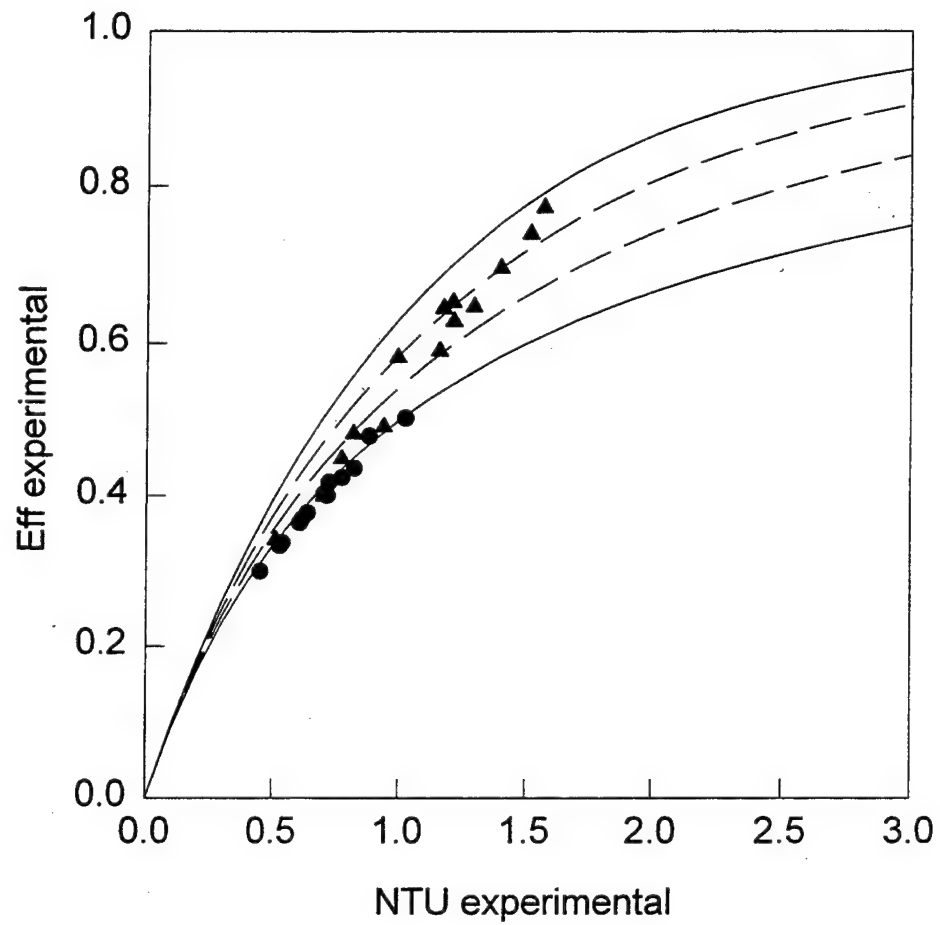


Figure 6.1 NTU vs. Effectiveness

NTU vs. Effectiveness

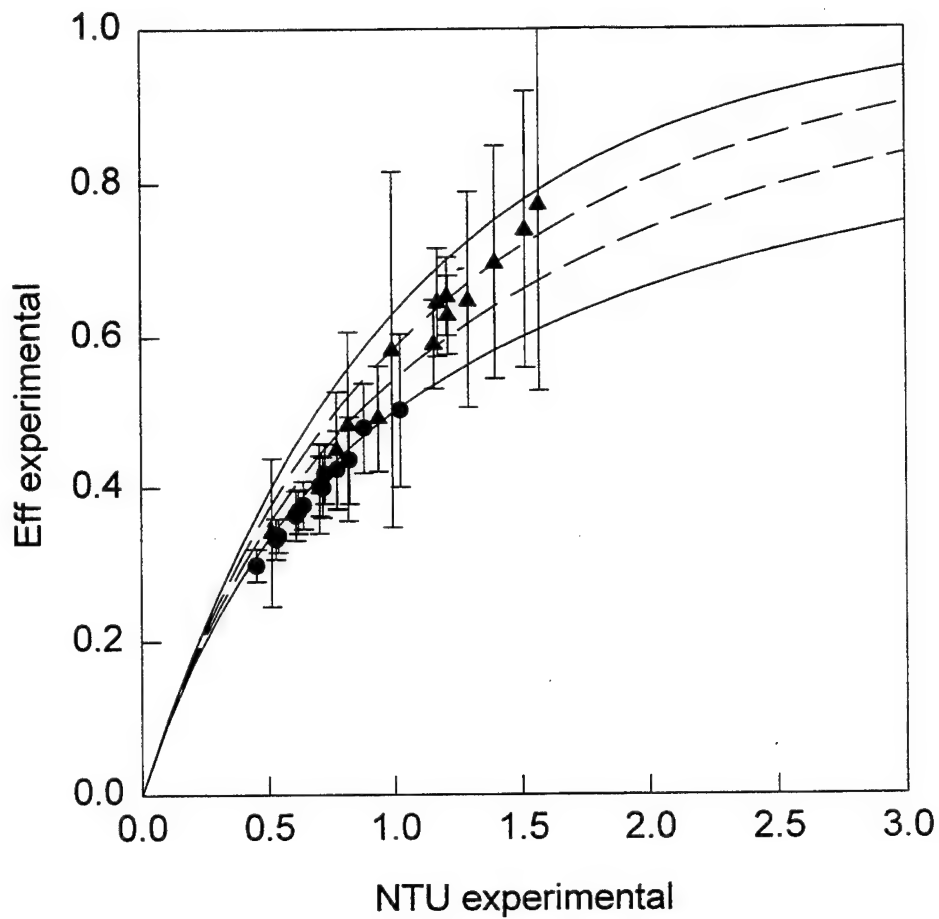


Figure 6.2 NTU vs. Effectiveness with error bars

VII. CONCLUSIONS AND RECOMMENDATIONS

The system design, component integration and performance analysis of the Superchanger plate and frame heat exchanger has been completed. Various performance characteristics were calculated from recommended correlations and measured experimental data. The overall heat transfer coefficient, the heat rate and the effectiveness of the heat exchanger were deduced from experimental data and compared to values calculated from correlations. The comparisons have been described earlier. From the discussion of the results it has been determined that the correlations can be used to predict the results of the heat exchanger satisfactorily. The expected values will be slightly higher than the experimental measurements. When the manufacturer's data was compared to the experimental data, it was found that the manufacturer's heat rate and heat transfer coefficient were also higher than the experimental results.

Additional data runs should be conducted with ethylene glycol as one of the operating fluids. This would allow for greater inlet ΔT 's and continuous cooling of the cold tank to maintain steadier temperatures. With the ability to continuously cool the cold tank, the length of each run would then be increased. With longer runs the insurance of steady state can be met.

APPENDIX A. STANDARD OPERATIONAL PROCEDURES FOR ALIGNMENT AND OPERATION OF THE SUPERCHARGER UX-056 PLATE AND FRAME HEAT EXCHANGER

HEAT EXCHANGER SYSTEM RECIRCULATION PROCEDURE (HESRP)

PROCEDURE

SYSTEM ALIGNMENT FOR RECIRCULATION

1. Conduct visual inspection of heat exchanger system and verify the following:
 - a. Ensure the deck are free of water and dry.
 - b. Inspect all piping runs and asccessories for loose connections, damage, or leaks.
 - c. Ensure all valve handles are installed and valve labels are in place.
 - d. Check water level in both tanks. Ensure enough water is present to support heat exchanger operations and ensure water level in hot water tank is above water level cutoff sensor on tank heater.
2. Ensure the following valves are in the fully open position:

a. Hot side pump suction valve	HW-1
b. Cold side pump suction valve	CW-1
c. Hot side recirculation valve	HW-3
d. Cold side recirculation valve	CW-3

3. Ensure the following valves are in the fully closed position:

- | | |
|---|------|
| a. Hot side pump discharge valve | HW-2 |
| b. Cold side pump discharge valve | CW-2 |
| c. Hot side heat exchanger discharge valve | HW-4 |
| d. Cold side heat exchanger discharge valve | CW-4 |
| e. Hot water tank drain valve | HW-5 |
| f. Cold water tank drain valve | CW-5 |

NOTE: Both drain valves must remain shut during operation of pumps and heat exchanger.

4. Start the cold side pump. Once pump has been started, slowly open pump discharge valve CW-2

5. Start the hot side pump. Once pump has been started, slowly open pump discharge valve HW-2

6. Monitor system for possible leaks.

HEAT EXCHANGER SYSTEM OPERATIONAL PROCEDURE (HESOP)

PROCEDURE

CAUTION

Check and maintain required water level in hot side water tank. Low water level could result in over heating of tank heater. Prior to operation of system monitor temperature of hot water tank to ensure no damage occurs to tank or tank heater.

SYSTEM ALIGNMENT FOR OPERATION

1. Align and place system in recirculation (HESRP)
2. Crack open cold side heat exchanger discharge valve CW-4.
3. Slowly close cold side recirculation valve CW-3.
4. Crack open hot side heat exchanger discharge valve HW-4.
5. Slowly close hot side recirculation valve HW-3.
6. Monitor system for possible leaks.
7. If leak occurs on hot side, stop hot side pump and close pump discharge valve HW-2.
8. If leak occurs on cold side, complete step 7. Then stop cold side pump and close pump discharge valve CW-2.

APPENDIX B. THERMOCOUPLE CALIBRATION

In the field of heat transfer it is vital that temperature measurements be accurate. To ensure accurate measurements are made, calibration of temperature reading devices are needed. This appendix outlines the procedure used in the calibration of the T-type thermocouples used in the experimental analysis of the Superchanger UX-056-UJ plate and frame heat exchanger.

The thermocouple wire was cut to the specified length. Beads were then made using a Dynatech Corporation Thermocouple Welder. The thermocouple beads were placed in a Keithly 740 System Scanning Thermometer. All beads were then immersed in a Rosemount Engineering Model 913A ethyl glycol bath. An associated Rosemont Engineering Model 920A commutating bridge provided the reference temperature as measured by a precision temperature probe. A four wire bridge electrical circuit was used to keep the lead resistance as low as possible.

The temperature of the ethyl glycol bath was slowly increased in small increments from roughly 15°C to 75°C . This covers the experimental temperature range of interest. When the temperature of the bath steadied out at each incremental change, the corresponding resistance from the commutating bridge and the reading from each channel on the thermometer scanner was recorded. Table B-1 lists all of the data recorded. The channel numbers correspond to individual thermocouple beads. The rough temp was used to make the incremental temperature changes.

The calibration of the T-type thermocouples yielded results within 0.1°C of the reference temperature up to a temperature of 50°C . Above that the readings were within 0.3°C of the reference temperature.

Trial #.	Channel Number										Resistance	Equly. Temp
	2	3	4	5	6	7	8	9	10	Rough Temp		
1	15.1	15.1	15.1	15.1	15.1	15.1	15.1	15.1	15.1	15	27.1051	15.13
2	18.2	18.2	18.2	18.2	18.2	18.2	18.2	18.2	18.2	18	27.4222	18.26
3	22.5	22.4	22.4	22.5	22.5	22.5	22.5	22.5	22.5	22	27.8534	22.51
4	23.5	23.5	23.5	23.5	23.5	23.5	23.5	23.5	23.5	23	27.9543	23.51
5	26.0	26.0	26.0	26.0	26.0	26.0	26.0	26.0	26.0	26	28.2128	26.07
6	31.3	31.3	31.3	31.3	31.3	31.3	31.3	31.3	31.3	30	28.7356	31.24
7	36.8	36.7	36.9	36.8	36.9	36.8	36.9	36.9	36.9	35	29.3005	36.84
8	43.0	43.0	43.1	43.0	43.1	43.0	43.1	43.1	43.1	40	29.9196	42.99
9	42.8	42.8	42.8	42.8	42.8	42.8	42.8	42.8	42.8	40	29.8952	42.75
10	48.3	48.4	48.4	48.3	48.4	48.4	48.4	48.3	48.4	45	30.4492	48.26
11	54.6	54.6	54.6	54.6	54.6	54.6	54.6	54.7	54.6	50	31.0755	54.50
12	54.3	54.3	54.3	54.3	54.3	54.3	54.3	54.3	54.3	50	31.0455	54.20
13	59.9	60.0	60.0	59.9	60.0	59.9	60.0	60.0	60.0	55	31.6097	59.84
14	67.8	67.9	67.9	67.8	67.9	67.8	67.9	67.9	67.9	60	32.3956	67.70
15	74.2	74.3	74.3	74.2	74.3	74.2	74.3	74.3	74.3	65	33.0336	74.10
16	81.4	81.5	81.5	81.4	81.5	81.4	81.5	81.6	81.6	70	33.7493	81.28
17	88.5	88.6	88.6	88.4	88.6	88.4	88.6	88.6	88.6	75	34.4543	88.38

APPENDIX C: UNCERTAINTY ANALYSIS

A. Velocity.

The equation for velocity is

$$u = \frac{\dot{m}}{\rho S} \quad (C.1)$$

where

$$\dot{m} = \frac{2\dot{M}}{N + 1} \quad (C.2)$$

and

$$\dot{M} = \rho Q \quad (C.3)$$

The uncertainty becomes

$$U_u = \sqrt{\left(\frac{\partial u}{\partial Q} U_Q \right)^2} \quad (C.4)$$

$$\frac{U_u}{u} = \frac{U_Q}{Q} \quad (C.5)$$

B. Reynold's Number

The Reynold's number equation is

$$Re = \frac{uD_h \rho}{\mu} \quad (C.6)$$

The uncertainty becomes

$$U_{Re} = \sqrt{\left(\frac{\partial Re}{\partial u} U_u \right)^2} \quad (C.7)$$

$$\frac{U_{Re}}{Re} = \frac{U_u}{u} \quad (C.8)$$

C. Nusselt Number

The Nusselt number equation is

$$Nu = 0.4 (Pr)^{0.4} (Re)^{0.64} \quad (C.9)$$

The uncertainty becomes

$$U_{Nu} = \sqrt{\left(\frac{\partial Nu}{\partial Re} U_{Re} \right)^2} \quad (C.10)$$

$$\frac{U_{Nu}}{Nu} = \frac{0.64}{Re} \frac{U_{Re}}{Re} \quad (C.11)$$

D. Heat Rate

The equation for the heat rate is

$$\dot{Q} = \dot{m}Cp (T_{h_i} - T_{h_o}) \quad (C.12)$$

The uncertainty becomes

$$U_{\dot{Q}} = \sqrt{\left(\frac{\partial \dot{Q}}{\partial \dot{m}} U_{\dot{m}}\right)^2 + \left(\frac{\partial \dot{Q}}{\partial T_{h_i}} U_{T_{h_i}}\right)^2 + \left(\frac{\partial \dot{Q}}{\partial T_{h_o}} U_{T_{h_o}}\right)^2} \quad (C.13)$$

$$\frac{U_{\dot{Q}}}{\dot{Q}} = \sqrt{\left(\frac{U_{\dot{m}}}{\dot{m}}\right)^2 + \left(\frac{U_{T_{h_i}}}{T_{h_i} - T_{h_o}}\right)^2 + \left(\frac{-U_{T_{h_o}}}{T_{h_i} - T_{h_o}}\right)^2} \quad (C.14)$$

E. Effectiveness

The equation for the effectiveness is

$$\epsilon = \frac{\dot{Q}}{\dot{Q}_{\max}} \quad (C.15)$$

The uncertainty becomes

$$U_{\epsilon} = \sqrt{\left(\frac{\partial \epsilon}{\partial \dot{Q}} U_{\dot{Q}}\right)^2 + \left(\frac{\partial \epsilon}{\partial \dot{Q}_{\max}} U_{\dot{Q}_{\max}}\right)^2} \quad (C.16)$$

and

$$\frac{U_{\epsilon}}{\epsilon} = \sqrt{\left(\frac{U_{\dot{Q}}}{\dot{Q}}\right)^2 + \left(\frac{U_{\dot{Q}}}{\dot{Q}_{\max}}\right)^2} \quad (C.17)$$

APPENDIX D. EXPERIMENTAL DATA

This appendix contains all pertinent data that was collected and the spread sheets that contain all the calculated parameters.

Run #	T1 (C)	T2 (C)	T3 (C)	T4 (C)	Freq Hz hot	Freq Hz cold	Flow rate hot (gpm)	Flow rate hot (m ³ /s)	Density Kg/m ³ hot	Viscosity Ns/m ² hot	Mass Flow rate hot (kg/s) Mdot h	Mass Flow rate per plate m dot/h	Flow rate cold (gpm)	Flow rate cold (m ³ /s)	Density Kg/m ³ cold
1	43.8	35.5	22.7	33.5	20	16	14.9740	0.000945	995.29	6.57E-04	0.940264	0.085479	11.9792	0.000756	995.500
2	43.0	34.3	24.0	31.8	23	22	17.2201	0.001086	995.31	6.70E-04	1.081323	0.098302	16.4714	0.001039	995.503
3	41.6	35.8	26.7	33.0	31	30	23.2097	0.001464	995.31	6.70E-04	1.457434	0.132494	22.4610	0.001417	995.469
4	42.5	36.9	29.1	34.2	33	35	24.7071	0.001559	995.29	6.57E-04	1.551434	0.141039	26.2045	0.001653	995.437
5	43.8	39.2	31.6	36.4	41	41	30.6967	0.001937	995.26	6.35E-04	1.927478	0.175225	30.6967	0.001937	995.395
6	43.2	40.0	34.2	37.8	46	45	34.4402	0.002173	995.26	6.33E-04	2.162532	0.196594	33.6915	0.002126	995.359
7	44.2	40.3	35.0	39.0	26	26	19.4662	0.001228	995.25	6.26E-04	1.222286	0.111117	19.4662	0.001228	995.341
8	42.8	35.3	25.6	33.5	22	22	16.4714	0.001039	995.3	6.65E-04	1.034302	0.094027	16.4714	0.001039	995.474
9	43.3	38.0	27.6	33.2	53	54	39.6811	0.002503	995.28	6.45E-04	2.491655	0.226514	40.4298	0.002551	995.459
10	42.6	39.4	31.4	35.1	88	84	65.8856	0.004157	995.27	6.41E-04	4.137062	0.376097	62.8908	0.003968	995.408
11	44.9	38.1	27.9	35	30	30	22.4610	0.001417	995.26	6.35E-04	1.410349	0.128214	22.4610	0.001417	995.438
12	46.3	40.1	29.5	36	40	42	29.9480	0.001889	995.23	6.15E-04	1.880409	0.170946	31.4454	0.001984	995.417
13	44.8	41.6	35.2	39	59	59	44.1733	0.002787	995.23	6.15E-04	2.773603	0.252146	44.1733	0.002787	995.343
14	42.0	32.9	23.9	33	14	15	10.4818	0.000661	995.33	6.86E-04	0.658211	0.059837	11.2305	0.000709	995.498
15	42.0	37.0	24.5	35	31	15	23.2097	0.001464	995.3	6.59E-04	1.457413	0.132492	11.2305	0.000709	995.468
16	42.9	39.4	25.1	37	48	15	35.9376	0.002267	995.27	6.39E-04	2.256573	0.205143	11.2305	0.000709	995.449
17	43.0	40.0	24.1	36	70	17	52.4090	0.003306	995.26	6.35E-04	3.290815	0.299165	12.7279	0.000803	995.462
18	41.7	39.8	25.6	36	93	17	69.6291	0.004393	995.27	6.44E-04	4.372142	0.397467	12.7279	0.000803	995.451
19	41.6	32.4	27.4	31.1	13	31	09.7331	0.000614	995.34	6.92E-04	0.611201	0.055564	23.2097	0.001464	995.479
20	41.9	32.7	28.7	31.1	13	49	09.7331	0.000614	995.34	6.88E-04	0.611197	0.055563	36.6863	0.002315	995.468
21	42.0	32.9	29.7	31.2	13	77	09.7331	0.000614	995.33	6.86E-04	0.611196	0.055563	57.6499	0.003637	995.458
22	45.6	36.9	23.8	32.9	31	32	23.2097	0.001464	995.27	6.38E-04	1.457368	0.132488	23.9584	0.001512	995.495
23	45.4	39.3	24.6	34.7	49	32	36.6863	0.002315	995.25	6.25E-04	2.303536	0.209412	23.9584	0.001512	995.472
24	44.3	40.4	27.1	36.1	68	32	50.9116	0.003212	995.25	6.25E-04	3.196743	0.290613	23.9584	0.001512	995.438
25	42.8	40.3	30.2	37.1	88	30	65.8856	0.004157	995.26	6.34E-04	4.137021	0.376093	22.4610	0.001417	995.401
26	30.1	23.5	21.4	22	10	85	07.4870	0.000472	995.52	8.60E-04	0.470240	0.042749	63.6395	0.004015	995.612
27	35.5	32	24.5	28	66	63	49.4142	0.003118	995.4	7.40E-04	3.103199	0.282109	47.1681	0.002976	995.532

Viscosity Ns/m ² cold	Mass Flow rate cold (kg/s) Mdot c	Mass Flow rate per plate mdot c	Velocity (m/s) hot	Velocity (m/s) cold	Reynold's number hot	Reynold's number cold	Prandtl number hot	Prandtl number cold	Nusselt number hot	Nusselt number cold	Heat Transfer Coefficient ch (w/m ² K)
8.35E-04	0.75237	0.06840	0.16256	0.13005	1,279.868	0,806.132	4.39	5.67	70.4095	58.0220	8,422.062
8.39E-04	1.03451	0.09405	0.18695	0.17882	1,443.568	1,103.514	4.45	5.67	76.4617	70.9367	9,145.992
8.04E-04	1.41064	0.12824	0.25197	0.24385	1,947.577	1,570.727	4.45	5.51	92.6148	87.9073	11,078.160
7.73E-04	1.64570	0.14961	0.26823	0.28449	2,113.818	1,904.789	4.39	5.21	97.0709	97.2517	11,611.173
7.36E-04	1.92774	0.17525	0.33326	0.33326	2,717.950	2,343.932	4.21	4.91	112.1211	108.4569	13,411.408
7.06E-04	2.11573	0.19234	0.37390	0.36577	3,055.160	2,679.752	4.2	4.71	120.7206	116.2114	14,440.043
6.92E-04	1.22240	0.11113	0.21133	0.21133	1,748.020	1,579.631	4.16	4.61	84.1254	82.1516	10,062.688
8.09E-04	1.03448	0.09404	0.17882	0.17882	1,391.600	1,144.368	4.41	5.55	74.4191	71.9879	8,901.675
7.94E-04	2.53913	0.23083	0.43080	0.43892	3,457.289	2,861.184	4.29	5.48	131.7752	128.7542	15,762.343
7.47E-04	3.94956	0.35905	0.71528	0.68277	5,778.732	4,728.059	4.23	5.04	182.0409	171.7233	21,774.892
7.74E-04	1.41060	0.12824	0.24385	0.24385	1,988.744	1,630.942	4.21	5.25	91.8043	88.3251	10,981.213
7.55E-04	1.97480	0.17953	0.32513	0.34138	2,737.163	2,339.448	4.04	5.12	110.7860	110.1541	13,251.712
6.94E-04	2.77392	0.25217	0.47956	0.47956	4,037.315	3,577.413	4.04	4.62	142.0731	138.7398	16,994.128
8.33E-04	0.70534	0.06412	0.11379	0.12192	0,858.205	0,757.427	4.62	5.66	55.6436	55.7141	6,655.829
8.03E-04	0.70532	0.06412	0.25197	0.12192	1,978.059	0,786.217	4.4	5.51	93.1181	56.4505	11,138.361
7.85E-04	0.70531	0.06412	0.39015	0.12192	3,161.011	0,804.231	4.22	5.29	123.6157	56.3490	14,786.339
7.98E-04	0.79936	0.07267	0.56897	0.13818	4,640.402	0,896.859	4.21	5.66	157.8950	62.0769	18,886.672
7.86E-04	0.79935	0.07267	0.75592	0.13818	6,078.126	0,909.509	4.28	5.29	188.9079	60.9648	22,596.291
8.14E-04	1.45768	0.13252	0.10567	0.25197	0,789.816	1,601.984	4.65	5.55	52.9002	89.2809	6,327.682
8.03E-04	2.30405	0.20946	0.10567	0.39828	0,794.539	2,568.309	4.63	5.51	53.0110	120.4189	6,340.933
7.93E-04	3.62061	0.32915	0.10567	0.62587	0,796.905	4,084.240	4.62	5.48	53.0661	161.6901	6,347.519
8.31E-04	1.50473	0.13679	0.25197	0.26010	2,045.354	1,621.224	4.23	5.63	93.6457	90.4821	11,201.470
8.07E-04	1.50469	0.13679	0.39828	0.26010	3,300.504	1,668.168	4.16	5.55	126.3539	91.6243	15,113.872
7.74E-04	1.50464	0.13679	0.55272	0.26010	4,580.292	1,739.671	4.16	5.25	155.8364	92.0498	18,640.432
7.41E-04	1.41055	0.12823	0.71528	0.24385	5,839.150	1,702.694	4.21	5.08	182.9096	89.6051	21,878.807
9.66E-04	3.99740	0.36340	0.08128	0.69090	0,489.384	3,702.709	4.17	5.11	37.2812	147.6661	4,459.408
8.70E-04	2.96254	0.26932	0.53646	0.51208	3,753.698	3,048.425	4.25	5.05	138.3788	129.7732	16,552.233

Heat Transfer Coefficient α_c (w/m ² ·K)	Plate Cond R_{wall}	Overall Heat Trans Coefficient U (w/m ² ·K)	$C_{p,h}$ J/kg·K	$C_{p,c}$ J/kg·K	C_h J/kg·K	C_c J/kg·K	C_{min}	Log mean Temp hot (°C)	Cr	Energy Balance Q _{dot,h} (W)	Energy Balance Q _{dot,c} (W)
6,940.330	3.95E-05	3,307.741	4179	4181	3,929.364	3,145.645	3,145.645	11.50476	0.80055	32,613.718	33,972.965
8,485.122	3.95E-05	3,749.660	4179	4180	4,518.849	4,324.243	4,324.243	10.74372	0.95693	39,313.986	33,729.093
10,515.069	3.95E-05	4,447.027	4179	4178	6,090.617	5,893.668	5,893.668	8.84765	0.96766	35,325.579	37,130.107
11,632.796	3.95E-05	4,726.170	4179	4178.5	6,483.444	6,876.547	6,483.444	8.04741	0.94283	36,307.287	35,070.391
12,973.118	3.95E-05	5,231.607	4179	4178	8,054.929	8,054.082	8,054.082	7.49956	0.99989	37,052.672	38,659.591
13,900.676	3.95E-05	5,534.315	4179	4178	9,037.221	8,839.529	8,839.529	5.59762	0.97812	28,919.107	31,822.306
9,826.594	3.95E-05	4,155.556	4179	4178	5,107.935	5,107.192	5,107.192	5.24984	0.99985	19,920.947	20,428.769
8,610.857	3.95E-05	3,731.749	4179	4178	4,322.346	4,322.046	4,322.046	9.49860	0.99993	32,417.597	34,144.165
15,400.988	3.95E-05	5,956.875	4179	4178	10,412.627	10,608.498	10,412.627	10.24927	0.98154	55,186.924	59,407.586
20,540.749	3.95E-05	7,456.667	4179	4178	17,288.782	16,501.266	16,501.266	7.74731	0.95445	55,324.103	61,054.886
10,565.045	3.95E-05	4,440.174	4179	4178	5,893.850	5,893.483	5,893.483	9.89697	0.99994	40,078.182	43,611.776
13,176.120	3.95E-05	5,239.530	4179	4178	7,858.228	8,250.707	7,858.228	10.44928	0.95243	48,721.015	53,629.595
16,595.411	3.95E-05	6,305.111	4179	4178	11,590.887	11,589.419	11,589.419	6.29947	0.99987	37,090.837	39,404.024
6,664.258	3.95E-05	2,942.921	4179	4178	2,750.663	2,946.921	2,750.663	9.24775	0.93340	25,031.031	25,343.519
6,752.348	3.95E-05	3,605.209	4179	4178	6,090.530	2,946.831	2,946.831	9.30052	0.48384	30,452.649	31,825.777
6,740.206	3.95E-05	3,913.995	4179	4178	9,430.220	2,946.776	2,946.776	9.62474	0.31248	33,005.768	34,477.278
7,425.351	3.95E-05	4,402.936	4179	4178	13,752.317	3,339.724	3,339.724	10.64554	0.24285	41,256.952	40,744.635
7,292.323	3.95E-05	4,527.231	4179	4178	18,271.181	3,339.685	3,339.685	9.24259	0.18278	34,715.244	35,066.696
10,679.366	3.95E-05	3,434.369	4179	4178	2,554.207	6,090.189	2,554.207	7.41302	0.41940	23,498.708	22,533.698
14,403.959	3.95E-05	3,750.504	4179	4178	2,554.194	9,626.315	2,554.194	6.84620	0.26533	23,498.582	23,103.157
19,340.623	3.95E-05	4,020.157	4179	4178	2,554.187	15,126.918	2,554.187	6.24797	0.16885	23,243.100	22,690.377
10,823.055	3.95E-05	4,521.422	4179	4178	6,090.339	6,286.748	6,090.339	12.89897	0.96876	52,985.951	57,209.402
10,959.675	3.95E-05	5,078.515	4179	4178	9,626.476	6,286.601	6,286.601	12.59431	0.65305	58,721.503	63,494.674
11,010.568	3.95E-05	5,435.708	4179	4178	13,359.191	6,286.382	6,286.382	10.54525	0.47057	52,100.845	56,577.440
10,718.151	3.95E-05	5,602.052	4179	4178	17,288.612	5,893.267	5,893.267	7.69138	0.34088	43,221.530	40,663.544
17,663.140	3.95E-05	3,121.487	4179	4178	1,965.133	16,701.129	1,965.133	4.37760	0.11766	12,969.880	13,360.903
15,522.867	3.95E-05	6,085.098	4179	4178	12,968.268	12,377.488	12,377.488	7.44989	0.95444	45,388.938	44,558.956

Qdot,max (W)	Imfd Qdot expected (W)	ϵ_h q/qmax hot eng bal	ϵ_c I/qmax col eng bal	NTU expected	NTU _h experimen	NTU _c experiment	E expected	E qexp/qmax	Uncertainty $\Delta E/E$	Uncertainty ΔE_h
66,373.108	45,139.668	0.49137	0.51185	1.29928	0.93873	0.97786	0.59729	0.68009	14.35%	0.070492
82,160.612	47,785.441	0.44769	0.41053	1.07143	0.88148	0.75626	0.52302	0.58161	12.51%	0.056008
87,815.649	46,670.951	0.40661	0.42282	0.93232	0.70567	0.74172	0.48626	0.53147	9.75%	0.039660
86,878.151	45,114.351	0.36950	0.40367	0.90071	0.72487	0.70018	0.48033	0.51928	9.29%	0.034309
98,259.794	46,539.291	0.46574	0.39344	0.80260	0.63899	0.66671	0.44526	0.47364	8.15%	0.037979
79,555.765	36,746.528	0.61548	0.40000	0.77360	0.60881	0.66993	0.43826	0.46190	8.77%	0.053963
46,986.169	25,877.627	0.26797	0.43478	1.00538	0.77395	0.79367	0.50136	0.55075	12.03%	0.032228
74,339.194	42,045.642	0.19830	0.45930	1.06685	0.82255	0.86636	0.51618	0.56559	13.13%	0.026037
163,478.247	72,420.331	0.29861	0.36340	0.70687	0.53866	0.57985	0.41572	0.44300	6.54%	0.019517
184,814.183	68,524.345	0.55220	0.33036	0.55835	0.45079	0.49748	0.36123	0.37077	7.03%	0.038808
100,189.216	52,125.637	0.30358	0.43529	0.93091	0.71575	0.77886	0.48212	0.52027	9.88%	0.029982
132,018.234	64,942.336	0.43791	0.40623	0.82385	0.61806	0.68033	0.45658	0.49192	7.77%	0.034035
111,258.419	47,113.566	0.74499	0.35417	0.67222	0.52921	0.56222	0.40200	0.42346	7.88%	0.058682
49,786.995	32,282.242	0.48538	0.50904	1.32197	1.02502	1.03782	0.58017	0.64841	20.32%	0.098641
51,569.546	39,772.850	0.58057	0.61714	1.51167	1.15742	1.20961	0.69606	0.77125	9.96%	0.057838
52,452.611	44,684.674	0.52290	0.65730	1.64117	1.21222	1.26627	0.75252	0.85191	8.21%	0.042921
63,120.786	55,598.016	0.76730	0.64550	1.62897	1.20878	1.19377	0.76265	0.88082	7.80%	0.059816
53,768.934	49,633.553	0.95714	0.65217	1.67498	1.17152	1.18338	0.78195	0.92309	10.96%	0.104873
36,269.745	30,198.932	0.69697	0.62128	1.66139	1.29277	1.23968	0.73661	0.83262	21.87%	0.152397
33,715.356	30,457.082	0.74797	0.68524	1.81433	1.39980	1.37625	0.79169	0.90336	21.87%	0.163547
31,416.498	29,794.148	0.17506	0.72224	1.94479	1.51716	1.48108	0.82920	0.94836	24.37%	0.042671
132,769.396	69,179.766	0.40521	0.43089	0.91731	0.70258	0.75858	0.48202	0.52105	14.68%	0.059466
130,761.309	75,868.277	0.54309	0.48558	0.99817	0.77257	0.83536	0.54396	0.58020	17.38%	0.094388
108,125.774	67,992.707	0.70165	0.52326	1.06841	0.81868	0.88903	0.58959	0.62883	25.98%	0.182261
74,255.167	51,109.352	0.58207	0.54762	1.17455	0.99327	0.93449	0.63941	0.68829	40.13%	0.233577
17,096.660	16,208.666	0.75862	0.78149	1.96269	1.57049	1.61784	0.84053	0.94806	32.09%	0.243418
136,152.366	53,773.270	0.33337	0.32727	0.60746	0.51274	0.50336	0.38117	0.39495	28.89%	0.096314

Uncertainty ΔE_c	U_{Ah} (exp) (W/K)	U_{Ac} (exp) (W/K)	U_h (exp) (W/m ² ·K)	NTU (exp)	E (exp)	Uncertainty $\Delta Q/Q$	Uncertainty $\Delta u/u$	Uncertainty $\Delta Re/Re$	Uncertainty $\Delta Nu/Nu$
0.073430	2,952.92	3,075.99	2,389.87	0.68288	0.42249	10.14%	10.00%	10.00%	6.40%
0.051359	3,811.72	3,270.23	3,084.92	0.64675	0.39608	8.85%	8.70%	8.70%	5.57%
0.041241	4,159.01	4,371.47	3,365.99	0.64148	0.39327	6.90%	6.45%	6.45%	4.13%
0.037482	4,699.66	4,539.55	3,803.54	0.58351	0.37239	6.57%	6.06%	6.06%	3.88%
0.032083	5,146.51	5,369.71	4,165.19	0.58222	0.36798	5.77%	4.88%	4.88%	3.12%
0.035070	5,381.59	5,921.85	4,355.44	1.05373	0.51596	6.20%	4.35%	4.35%	2.78%
0.052290	3,952.69	4,053.45	3,199.00	0.91454	0.47770	8.50%	7.69%	7.69%	4.92%
0.060307	3,555.09	3,744.43	2,877.21	0.34142	0.25452	9.28%	9.09%	9.09%	5.82%
0.023752	5,608.83	6,037.79	4,539.36	0.33990	0.25427	4.62%	3.77%	3.77%	2.42%
0.023218	7,438.62	8,209.12	6,020.25	1.26218	0.56506	4.97%	2.27%	2.27%	1.45%
0.042991	4,218.27	4,590.19	3,413.95	0.53680	0.34930	6.98%	6.67%	6.67%	4.27%
0.031573	4,856.89	5,346.22	3,930.80	0.41908	0.29740	5.50%	5.00%	5.00%	3.20%
0.027897	6,133.26	6,515.76	4,963.79	2.22974	0.69041	5.57%	3.39%	3.39%	2.17%
0.103448	2,819.50	2,854.70	2,281.88	0.96679	0.49696	14.37%	14.29%	14.29%	9.14%
0.061481	3,410.72	3,564.52	2,760.38	1.15744	0.61296	7.04%	6.45%	6.45%	4.13%
0.053953	3,572.15	3,731.41	2,891.02	1.06959	0.61240	5.80%	4.17%	4.17%	2.67%
0.050321	4,036.99	3,986.86	3,267.23	1.20879	0.66416	5.51%	2.86%	2.86%	1.83%
0.071458	3,912.51	3,952.12	3,166.49	1.53179	0.75339	7.75%	2.15%	2.15%	1.38%
0.135846	3,302.00	3,166.40	2,672.39	1.29278	0.65824	15.46%	15.38%	15.38%	9.85%
0.149831	3,575.37	3,515.20	2,893.63	1.39981	0.70976	15.46%	15.38%	15.38%	9.85%
0.176046	3,875.11	3,782.96	3,136.22	0.63627	0.45609	17.24%	15.38%	15.38%	9.85%
0.063235	4,278.92	4,619.99	3,463.03	0.68064	0.40756	10.38%	6.45%	6.45%	4.13%
0.084393	4,856.82	5,251.60	3,930.73	0.77259	0.46979	12.29%	4.08%	4.08%	2.61%
0.135922	5,146.55	5,588.75	4,165.23	0.87329	0.52612	18.37%	2.94%	2.94%	1.88%
0.219754	5,853.62	5,507.19	4,737.48	0.99327	0.58380	28.38%	2.27%	2.27%	1.45%
0.250756	3,086.23	3,179.27	2,497.76	1.57049	0.77259	22.69%	20.00%	20.00%	12.80%
0.094552	6,346.42	6,230.37	5,136.31	0.51274	0.34157	20.43%	3.03%	3.03%	1.94%

LIST OF REFERENCES

1. Tranter, Superchanger Installation and Operation Manual, 1994
2. Gupta, J. P., *Fundamentals of Heat Exchanger and Pressure Vessel Technology*, Hemisphere Publishing Corporation, 1986
3. Kays, W. M. and London, A. L., *Compact Heat Exchangers*, McGraw-Hill, Inc., 1984
4. Chisholm, D., *Developments in Heat Exchanger Technology - I*, Applied Science Publishers, 1980
5. Hewitt, G. F. and Shires, G. L. and Bott, T.R., *Process Heat Transfer*, CRC Press, Inc., 1994
6. Omega, Model FP-6000 Operator's Manual, 1995
7. Streeter, V. L. and Wylie, E. B., *Fluid Mechanics* 8th edition, McGraw Hill, 1985
8. Incropera, F. P. and DeWitt, D. P., *Introduction to Heat Transfer*, John Wiley and Sons, Inc., 1990
9. Hurley, J., 1996, "Analysis of Steam and Hydronic compartment heating systems aboard U.S. Coast Guard 140 Foot WTGB Class Cutters", Master's Thesis, Naval Postgraduate School, Monterey, CA

INITIAL DISTRIBUTION LIST

1. Defense Technical Information Center 2
8725 John J. Kingman Road, Ste 0944
Ft. Belvoir, Virginia 22060-6218
2. Dudley Knox Library 2
Naval Postgraduate School
411 Dyer Road
Monterey, California 93943-5101
3. Mechanical Engineering Curricular Office, Code 34 1
Naval Postgraduate School
Monterey, California 93943-5101
4. Assistant Professor Ashok Gopinath 1
Mechanical Engineering Department, Code ME/Gk
Naval Postgraduate School
Monterey, California 93943-5101
5. LT Darren R. Plath 3
SRF Yokosuka
PSC 473 Box 8-15
FPO AP 96349-1400